



Co-culturing bacteria with monospecific microalgal biofilms for improved biomass and lipid production

Nadeeshani Dehel Gamage^{a,*}, Aurélie Mossion^a, Murtaza Khan^a, Rejaul Karim^a, Vony Rabesaotra^a, Gaëtane Wielgosz-Collin^a, Thierry Lebeau^b, Vona Méléder^{a,c}

^a Nantes Université, Institut des Substances et Organismes de la Mer, ISOMer, UR 2160, F-44000 Nantes, France

^b Nantes Université, Laboratoire de Planétologie et Géosciences, UMR LPG-Nantes 6112 CNRS, 2 rue de la Houssinière, BP, 92208, 44322 Nantes Cedex, France

^c Institut Universitaire de France (IUF), 103 Boulevard Saint-Michel, 75005 Paris, France

ARTICLE INFO

Keywords:

Benthic diatoms
Microalgal biofilms
Porous substrate photobioreactor (PSBR)
Microalgae-bacteria interaction
Co-culturing
Biomass production
Lipid production

ABSTRACT

Integrating microbiome engineering into microalgal biofilms could offer an environmentally sustainable and economically viable strategy to enhance biomass and lipid yields while leveraging the inherent advantages of biofilm-based systems. Building on this hypothesis, our objective was to improve biomass and lipid production in the naturally biofilm-forming marine benthic diatom, *Amphora* sp. (NCC169) by co-culturing it with two of its native biofilm associated bacteria, *Nitratireductor* sp. and *Sulfitobacter* sp., in a vertical porous substrate biofilm photobioreactor (PSBR) operated in batch mode. Axenic, non-axenic, and co-cultures were maintained in triplicate for 15 days in F/2 enriched artificial seawater at 18 ± 1 °C under continuous light ($100 \mu\text{mol photons.m}^{-2} \text{ s}^{-1}$). Biomass and lipid content were quantified gravimetrically, followed by fatty acid profiling via gas chromatography-mass spectrometry (GC-MS) at three harvesting days (3, 6, and 15). Results showed that the *Amphora*-*Nitratireductor* co-culture achieved the highest surface biomass ($2.54 \pm 0.39 \text{ g.m}^{-2}$) and productivity ($0.99 \pm 0.26 \text{ g.m}^{-2}.\text{day}^{-1}$) on day 3, further peaking on day 6 ($7.27 \pm 1.31 \text{ g.m}^{-2}$; $1.24 \pm 0.16 \text{ g.m}^{-2}.\text{day}^{-1}$) and were significantly different from the non-axenic control. The *Amphora*-*Sulfitobacter* co-culture recorded a significantly higher lipid yield on day 3 ($1.51 \pm 0.31 \text{ g.m}^{-2}$), surpassing axenic cultures by 3-fold, non-axenic by 6-fold, and *Amphora*-*Nitratireductor* by 5-fold, with a lipid content of $67.03 \pm 17.80\%$ of *Amphora* dry biomass weight. The fatty acid profile of *Amphora* sp. remained largely consistent across culture conditions and harvest days, dominated by palmitic acid (16:0) and palmitoleic acid (16:1), with low polyunsaturated fatty acid levels, highlighting its potential for pharmaceutical, nutraceutical, cosmetic, and bioenergy applications.

1. Introduction

Microalgal biofilms have gained increasing attention over the past two decades as a promising alternative to suspended microalgal cultivation systems (Gross et al., 2013, 2015; Berner et al., 2015; Ennaceri et al., 2023; Arnaldo et al., 2024a). Unlike suspended cultures, which rely on energy-intensive harvesting techniques such as centrifugation and filtration, biofilm cultures enable easier biomass recovery through scraping (Osorio et al., 2021) or surface vacuuming (Berner et al., 2015). This approach can significantly reduce harvesting costs, which may comprise up to 25% of total production expenses (Arnaldo et al., 2024a and b). Additionally, biofilm cultures require less water and enable

denser microalgal production in a more compact area compared to suspended cultures (Cheah and Chan, 2021; Ennaceri et al., 2023). In particular, vertically scalable algal biofilms have demonstrated higher lipid productivity than conventional terrestrial biofuel crops (Schnurr and Allen, 2015), making them a more efficient and cost-effective platform for biomass recovery and metabolite production (Mantzorou and Verweridis, 2019; Osorio et al., 2021; Vale et al., 2023). However, despite these advantages, the broader biotechnological potential of microalgal biofilms remains underexplored, with most research focusing on applications in wastewater treatment (Ennaceri et al., 2023).

Enhancing biomass and lipid yields in microalgal biofilms can be achieved through various strategies, including the use of efficient

* Corresponding author.

E-mail addresses: nadeeshani.dehel-gamage@univ-nantes.fr (N.D. Gamage), Aurelie.Mossion@univ-nantes.fr (A. Mossion), murtaza.khan@etu.uca.fr (M. Khan), karim.rejaul@etu.univ-nantes.fr (R. Karim), Vony.Rabesaotra@univ-nantes.fr (V. Rabesaotra), Gaetane.Wielgosz-Collin@univ-nantes.fr (G. Wielgosz-Collin), thierry.lebeau@univ-nantes.fr (T. Lebeau), vona.meleder@univ-nantes.fr (V. Méléder).

<https://doi.org/10.1016/j.jbiotec.2026.03.007>

Received 12 November 2025; Received in revised form 5 March 2026; Accepted 7 March 2026

Available online 11 March 2026

0168-1656/© 2026 The Author(s). Published by Elsevier B.V. This is an open access article under the CC BY license (<http://creativecommons.org/licenses/by/4.0/>).

biofilm reactor designs (Podola et al., 2017), manipulation of eco-physiological conditions (e.g., nutrient limitation, light intensity, carbon sources, salinity, and temperature), and advanced bio-engineering approaches (e.g., metabolic or genetic) (González-González, De-Bashan, 2021; Palacios et al., 2022). Among the various biofilm cultivation systems, porous substrate bioreactors (PSBRs) feature a unique configuration that enables complete separation of algal biomass from the liquid culture medium (Schultze et al., 2015; Podola et al., 2017). In PSBRs, microalgae grow on a hydrophilic, porous, thin sheet-like substrate in direct contact with the ambient gas phase, while essential substances such as water, nutrients, and gases diffuse through the substrate and reach the biofilm via diffusion and evaporative flux (Podola et al., 2017; Arnaldo et al., 2024a). Between horizontal and vertical PSBR configurations, the latter is gaining increasing attention for its space utilization efficiency and light diffusion capacity (Podola et al., 2017; Arnaldo et al., 2024b). In general, PSBRs offer high light utilization efficiency and efficient gas exchange, thereby enhancing the photosynthetic efficiency and biomass productivity of microalgal cells (Podola et al., 2017). Beyond increased biomass, PSBRs have also demonstrated higher lipid productivity in certain microalgal strains, including *Nannochloropsis oculata* ($1.33 \text{ g.m}^{-2}.\text{day}^{-1}$, lipid content 21.9% w/w) (Tran et al., 2022) and *Ettlia* sp. ($4.2 \pm 0.3 \text{ g.m}^{-2}.\text{day}^{-1}$) (Kim et al., 2018) under optimised culture conditions. Taken together, PSBRs offer a favourable energy balance by reducing water use, avoiding intensive harvesting, and using low-pressure systems, making them a promising option for cost-effective and sustainable microalgal biofilm biotechnology (Podola et al., 2017; Arnaldo et al., 2024a).

In parallel, recent advances in microalgal biotechnology, including microbiome engineering, genetic modification, and omics-based approaches (e.g., metabolomics and transcriptomics) (Lian et al., 2018; Kumar et al., 2020) offer promising alternatives for enhancing biofilm productivity. Despite the complexity of these methods, they could offer more efficient solutions compared to conventional eco-physiological modifications, which often induce stress and result in reduced biomass yields (Kumar et al., 2020). Of these approaches, microbiome engineering stands out as an environmentally sustainable strategy for microalgal biofilms, as it can mimic the naturally complex and dynamic biofilm environment characterized by diverse interactions with other microbes, primarily bacteria (Ramanan et al., 2016; Wang et al., 2022; Ennaceri et al., 2023). Moreover, the co-occurrence of bacteria in microalgal biofilms is often inevitable due to the elevated production of extracellular polymeric substances (EPS), which act as chemoattractants (Lipsman et al., 2024). The most common strategies in microbiome engineering for microalgal biotechnology such as co-culturing and manipulating natural microbiomes (Vrieze et al., 2017) have been successfully applied in suspended microalgal cultures. For instance, *Chlorella vulgaris* and *Phaeodactylum tricornutum* co-cultured with bacterial strains from genera such as *Bacillus*, *Rhizobium*, and *Marinobacter* have demonstrated enhanced biomass and lipid yields through nutrient recycling and metabolite exchange, with potential applications in nutraceuticals, pharmaceuticals, and biofuels (Nascimento et al., 2013; Cho et al., 2015; Wang et al., 2015; Chorazyczewski et al., 2021; Sittmann et al., 2021). These approaches offer simplified, scalable models to study microalgae-bacteria interactions by reducing the complexity of natural multispecies interactions (Rasheed et al., 2023), enabling clearer insight into their functions and enhancing biomass and metabolite production for industrial applications (Ramanan et al., 2016; Tong et al., 2023). However, such studies on microalgal biofilms are scarce.

Benthic diatoms, an underexplored group of microalgae in biotechnology, have recently attracted attention for their high levels of economically valuable lipids and their strong adaptation to biofilm systems, where they often outperform suspension cultures (Boukhris et al., 2017; Cointet et al., 2019, 2021). As natural biofilm formers, their physiological performance is closely linked to interactions with associated microorganisms, bacteria (Koedooder et al., 2019). Based on these attributes, we hypothesized that benthic diatoms are ideal candidates

for exploring microalgal biofilm-bacterial co-culture strategies. *Amphora* sp. is a biofilm forming benthic diatom with lipid content exceeding 20% of its dry biomass (Cointet et al., 2019). However, due to its sessile, benthic nature, *Amphora* sp. performs poorly in suspension-based systems such as airlift photobioreactors (Cointet et al., 2021), but demonstrates improved growth, biomass accumulation, and lipid content reaching up to 27% under PSBR-based biofilm cultivation (Arnaldo et al., 2024a). Accordingly, to test our hypothesis, this model benthic diatom strain was chosen for binary co-cultivation with two of its phycosphere-associated bacteria in a laboratory scale vertical PSBR operated in batch mode, with the objective of enhancing *Amphora* sp. biomass and lipid yields. The bacterial strains *Nitratireductor* sp. and *Sulfitobacter* sp. were selected based on our preliminary work, in which they were the only isolates that did not negatively affect *Amphora* sp. biomass among several binary co-cultures tested in bottle flasks (Gamage et al., 2026). Growth monitoring and photosynthetic performance were assessed using spectroradiometry (Normalised difference vegetation index, NDVI) and pulse amplitude modulation (PAM) fluorometry (the maximum photosynthetic efficiency, F_v/F_m), respectively, followed by measurements of biomass accumulation and lipid production at multiple time points against axenic and non-axenic controls. This study demonstrates the potential of bacterial-benthic diatom biofilm co-cultures in a vertical PSBR to enhance biomass and lipid production, with implications for future lipid-based biotechnological applications.

2. Materials and methods

2.1. Culture preparation and maintenance

2.1.1. Axenic and non-axenic *Amphora* sp. cultures

Amphora sp. is a benthic diatom strain isolated from the Northwest French Atlantic coast (47°22'06" N, 02°32'52" W) and has been maintained long-term under non-axenic conditions at the ISOMer laboratory, Nantes University, under the code NCC169. The strain is currently preserved in the Roscoff Culture Collection (RCC) under the accession code RCC5813. In this study, the stock culture of non-axenic *Amphora* sp. was maintained in 250 mL culture flasks containing artificial seawater (ASW-salinity- 28‰; pH- 7.8, see Supplementary I) enriched with F/2 medium, incubated at 16 °C under a 12:12 light-dark cycle with a photon flux density of $100 \mu\text{mol photons.m}^{-2}.\text{s}^{-1}$.

Axenic *Amphora* sp. cultures were derived from the non-axenic stock using an antibiotic-antimycotic solution at a concentration of 10 mL per liter (containing 10,000 units of penicillin, 10 mg of streptomycin, and 25 μg of amphotericin B per mL; BioReagent, A5955 SIGMA) as described by Lépinay et al. (2016). Three repetitive treatments were performed at one-week intervals, and the absence of bacterial contamination was confirmed after each treatment by streaking on agar plates. The axenic *Amphora* sp. cultures were also maintained under the same conditions as the non-axenic *Amphora* sp. cultures.

2.1.2. Bacteria cultures

Nitratireductor sp. and *Sulfitobacter* sp. were previously isolated (see Supplementary II for the closest related species names and sequence similarity) and identified from the biofilm of non-axenic *Amphora* sp. In our preliminary co-culture studies conducted in bottle culture flasks with axenic *Amphora* sp., these two-biofilm forming bacterial strains exhibited a neutral effect on both biomass and lipid production, whereas all other biofilm-associated bacteria (*Maribacter* sp., *Pseudomonas* sp., *Janibacter* sp., *Brevundimonas* sp., *Aureimonas* sp., and *Erythrobacter*) negatively impacted biomass production (Gamage et al., 2026). Based on these findings, *Nitratireductor* sp. and *Sulfitobacter* sp. were selected for co-culture with axenic *Amphora* sp. in a biofilm-based vertical PSBR, a more efficient system than bottle flasks. The previously isolated and purified strains were cultured in 4 mL of liquid marine broth (Difco™2216, USA) at 18–19 °C for 48 h, then stored at –80 °C with 30% glycerol until use in co-culture experiments.

2.2. Cell enumeration

For disc inoculation, *Amphora* sp. cells and bacterial cells were counted using a Neubauer hemocytometer (MARIENFELD, Germany) and the colony-forming unit (CFU) method, respectively. *Amphora* sp. cells were counted from starter cultures following homogenization under an optical microscope (OLYMPUS CH40, Japan, $\times 40$ objective). For bacteria, 100 μL of each stock culture was serially diluted (10^{-1} to 10^{-5}), and 25 μL of each dilution was plated onto marine agar. Further, to monitor bacterial growth in co-cultures with axenic *Amphora* sp. in the PSBR, a biofilm disc was transferred to 1 mL of ASW and vortexed for 30 s. The resulting suspension was serially diluted (10^{-1} to 10^{-5}) and plated on marine agar. All plates were incubated in the dark at 20 °C for one week, and bacterial abundance was expressed as CFUs per square meter.

2.3. Experimental setup

2.3.1. Disc inoculation

Microfiber filters (\varnothing 25 mm, 1.2 μm pore size, Whatman™ GF/C, China) were used as growth substrates for *Amphora* sp. in the vertical biofilm PSBR system. To establish a stable biofilm of axenic, non-axenic, and bacterial co-cultures of *Amphora* sp. on filter discs, a 4-day incubation was carried out outside the PSBR (Fig. 1). For this, pre-combusted (at 400 °C for 4 h) and pre-weighed discs were inoculated with 2×10^6 cells in 2 mL of ASW in 6-well tissue culture plates (Dutscher, China) and incubated at 18 ± 1 °C under continuous white light (100 $\mu\text{mol photons.m}^{-2}\text{s}^{-1}$). For co-cultures, axenic *Amphora* sp. and bacteria (*Nitratireductor* sp./ *Sulfitobacter* sp.) were inoculated at a 10:1 cell ratio (2×10^6 *Amphora* sp. cells: 2×10^5 bacteria cells per disc). To achieve the desired number of bacterial cells, small aliquots from the stock bacteria cultures were diluted in sterilized ASW. In total, 30 discs were used for a trial. Every handling was done aseptically.

2.3.2. PSBR launch

The detailed configuration and startup procedure of our laboratory scale vertical biofilm PSBR system have been described by Arnaldo et al. (2024a). Briefly, this customized PSBR (based on the Nano model by Synoxis Algae, France) was specifically designed for benthic diatom biofilm cultivation. It comprises two vertical polymethyl methacrylate (PMMA) chambers, each 40 cm in height and 5 cm in inner diameter, with a total volume of 785 mL. The chambers provide approximately 98% light transmission. One chamber serves as a reservoir for the culture medium, while the other functions as a growth chamber equipped with a metal plate supporting inoculated glass microfiber discs for biofilm development. A sparger at the top regularly wets the biofilm with medium from the reservoir. The pH in the reservoir is automatically maintained at 7.8 through on-demand CO₂ injection triggered by pH fluctuations; therefore, the exact volume of CO₂ injected is not

measured. An outflow valve recirculates the medium back to the reservoir. Light (400–700 nm, maximum $\sim 300 \mu\text{mol photons.m}^{-2}\text{s}^{-1}$) is supplied by an adjustable LED panel. CO₂ delivery, medium flow, and lighting are programmed via an integrated control system.

Prior to each experiment, the PSBR components (e.g., PMMA chambers, nutrient sparger, connecting valves, and tubes) were sterilized according to the manufacturer's instructions. After sterilization, the components were assembled in a sterile environment, and both cylinders were sealed with 0.2 μm air filters (\varnothing 25 mm, VWR®, China) to prevent contamination. Calibration of the pH probe and dosing pumps was performed before each run. Light intensity was maintained at 100 $\mu\text{mol photons.m}^{-2}\text{s}^{-1}$, using a mix of 25% green, 25% red, and 27% blue light fluxes. Pre-incubated discs were aseptically attached to the PSBR's metal plate, which was wrapped with a thin layer of tissue paper using water capillary action. The metal plate with the discs was then inserted into the growth chamber, while the reservoir chamber was filled with 700 mL of culture medium. The medium was dispersed via a nutrient sparger located above the metal disc holder at a rate of 1 mL every 5 min, while the accumulated medium in the growth chamber was recirculated to the reservoir at a rate of 8 mL every 5 min. The room temperature during operations was at 18 ± 1 °C.

2.4. Ecophysiology survey

Axenic and non-axenic *Amphora* sp. (with native microbiota) were used as controls. All cultures, including two co-cultures of axenic *Amphora* sp. with *Nitratireductor* sp. and *Sulfitobacter* sp., were cultivated in the biofilm PSBR for an initial 15-day period, followed by separate 6-day cultures. All experiments were conducted in triplicate as independent sequential runs, as simultaneous triplicate operation was not feasible due to the use of a single PSBR. The 15-day cultures were used to assess growth curves under the provided conditions, while the 6-day cultures were conducted to obtain additional biomass representative of the exponential growth phase.

Non-destructive reflectance-based and chlorophyll-a fluorescence methods were used to assess the biomass and photosynthetic efficiency of *Amphora* sp. biofilms under axenic, non-axenic, and co-culture conditions in the biofilm PSBR. Measurements were taken with minimal disturbance to the biofilms at regular intervals on different days (e.g., days 0, 2, 5, 7, 9, 13, and 15) throughout the cultivation period. All handling procedures, including the removal of the metal plate with discs from the PSBR cylinder, were conducted in a pseudo-aseptic environment. Additionally, calibration experiments were carried out to convert biomass proxies obtained from reflectance-based measurements into approximate cell numbers of *Amphora* sp. per square meter.

2.4.1. Growth survey

NDVI, which is proportional to chlorophyll-a content, was used as a proxy for biomass (Cointet et al., 2019). As culture conditions were

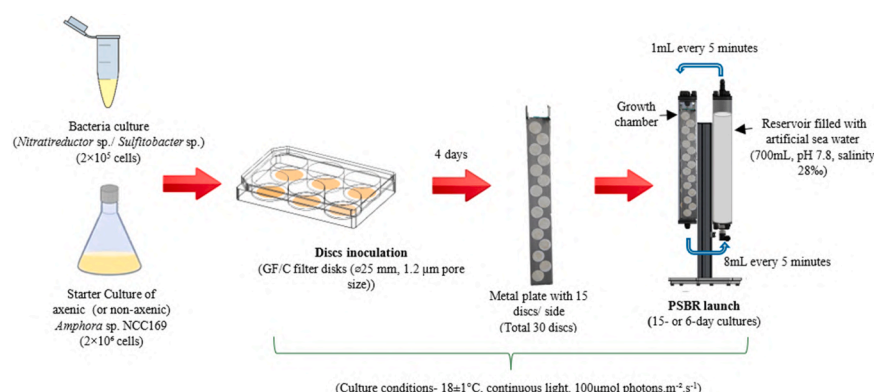


Fig. 1. Schematic illustration of the experimental setup, including disc inoculation and operation of the vertical biofilm PSBR.

identical across treatments, temporal changes in NDVI of *Amphora* sp. in each culture were interpreted as reflecting changes in *Amphora* growth. To calculate NDVI (Eq. 1), the reflectance (ρ) of the biofilm was measured across the wavelength (λ) range of 340–1025 nm using a spectroradiometer, equipped with a 3 mm diameter fibre optic probe (JAZ-VIS-NIR, Ocean Insights) and a 40 W halogen light source (OSRAM, France). Prior to each measurement, the spectroradiometer was calibrated using a white reference standard (WS-1-SL Spectralon Reflectance Standard, Ocean Insights) representing 100% reflectance. The probe was positioned approximately 0.5 cm from the biofilm surface, perpendicular (90°) to the discs, covering an estimated measurement area of 0.3 cm². Reflectance spectra were recorded at a minimum of 10 positions across the biofilm surface on 10 randomly selected discs. The average NDVI value for each sampling day was then calculated from the collected reflectance spectra, using the reflectance in the red ($\rho_{\lambda 675}$) and near infra-red ($\rho_{\lambda 750}$) domains. Further, the relative growth rate (μ) was calculated based on the NDVI values corresponding to the beginning (t_1) and late exponential phase (t_2), as shown in Eq. 2.

$$\text{NDVI} = \frac{\rho_{\lambda 750} - \rho_{\lambda 675}}{\rho_{\lambda 750} + \rho_{\lambda 675}} \quad (1)$$

$$\mu = \frac{\ln(\text{NDVI}t_2) - \ln(\text{NDVI}t_1)}{t_2 - t_1} \quad (2)$$

2.4.2. Photosynthetic efficiency measurements

The photosynthetic efficiency of *Amphora* sp. biofilms under each culture condition was measured using PAM fluorometry (Water-PAM, Walz, Germany). The fibre optic probe was positioned approximately 0.5 cm from the biofilm surface, perpendicular (90°) to the discs. A minimum of 10 measurements were taken across the biofilm surface of each of 10 randomly selected discs. Prior to each measurement, the metal plate with discs was dark-adapted for 15 min to ensure that all photosystem II (PSII) reaction centres were fully open. A weak, non-actinic measuring light ($\sim 0.8 \mu\text{mol photons.m}^{-2}.\text{s}^{-1}$) was initially used to record the minimum fluorescence yield (F_0), followed by a saturating light pulse ($2500 \mu\text{mol photons.m}^{-2}.\text{s}^{-1}$ for 0.8 s) that temporarily halted electron transport, causing all absorbed light energy to be emitted as fluorescence (Sapp et al., 2007). The maximum photosynthetic efficiency of PSII (F_v/F_m) was then calculated (Eq. 3). F_v/F_m values between 0.5 and 0.7 were considered indicative of non-stressed, physiologically healthy cells (Rijstenbil, 2003; White et al., 2011).

$$\frac{F_v}{F_m} = \frac{(F_m - F_0)}{F_m} \quad (3)$$

2.4.3. Biomass calibration experiment

Three axenic *Amphora* cultures grown in Erlenmeyer flasks under the conditions described in Section 2.1.1 were counted to obtain concentrations ranging from 2×10^6 – 10×10^6 cells. These concentrations were then filtered through microfiber filters (\varnothing 25 mm, 1.2 μm pore size, Whatman™ GF/C, China) to achieve a homogeneous distribution on the discs. Reflectance measurements were recorded at 10 random positions on each filter to construct a calibration curve between cell number and NDVI. The resulting equation, $\text{NDVI} = 0.1042 \times (\text{cells} \times 10^{10} \text{ per m}^2) + 0.1681$ ($R^2 = 0.96$, see Supplementary III), was applied to convert NDVI values of *Amphora* in co-cultures for estimating the *Amphora*: bacteria ratio at days 3, 6 and 15. However, conversion to cell numbers was not applied for growth curves assessment because the calibration did not adequately capture the lower concentration range of *Amphora* cells (0.5 – 1×10^6). This limitation resulted in negative values when applying the equation to day 0 measurements in PSBR cultures.

2.5. Nutrient analysis

Nutrient consumption by axenic, non-axenic, and co-cultured *Amphora* sp. was assessed at the beginning and end of both the 15-day and

6-day culture periods. Concentrations of dissolved inorganic nitrogen ($\text{DIN} = \text{NO}_3^- + \text{NO}_2^-$), dissolved inorganic phosphorus ($\text{DIP} = \text{PO}_4^{3-}$), dissolved silicate ($\text{DSi} = \text{Si}(\text{OH})_4^-$), and ammonium (NH_4^+) were determined using colorimetric methods described by Aminot and Kérouel (2007). DIN, DIP and DSi were analysed using SEAL Analytics AA3 Autoanalyzer. The limits of quantification were 0.2 μM for DIN, 0.05 μM for DIP, and 0.4 μM for DSi. Ammonium was quantified using a UV–VIS spectrophotometer (UV-1900, SHIMADZU, Japan). The average nutrient concentrations were calculated as follows, for day 0, from both 15-day and 6-day cultures; for day 6, from 6-day cultures; and for day 15, from 15-day cultures, under the corresponding culture condition. However, nutrient data for non-axenic *Amphora* sp. over the 15-day culture period were not available for comparison, since nutrient analysis was initiated only after completion of the 15-day cultivation in the PSBR. Thus, nutrient data for non-axenic *Amphora* sp. were presented only based on 6-day cultures.

2.6. Harvesting and biomass analysis

Harvesting was performed at the end of both the 15-day and 6-day cultivation periods. Additionally, samples were collected on day 3 from the 6-day cultures. Thus, day 3 generally corresponds to the exponential growth phase, while day 6 and day 15 are indicative of the late exponential or early stationary phase and the stationary phase, respectively, depending on the culture condition. For each condition (axenic, non-axenic, and the two co-cultures), 10 discs were randomly selected for biomass analysis, followed by lipid analysis. The discs were washed with 10 mL of ammonium formate (NH_4HCO_2) to remove salt residues and then freeze-dried at -50°C (Heto FD 3, Thermo Fisher Scientific, France) for two days. If freeze-drying could not be carried out immediately after washing, the discs were stored at -80°C . The lyophilized discs were weighed using an analytical balance (Explorer EX125, Ohaus Explorer® semi-micro analytical balance, France). Surface biomass production (g.m^{-2}) was calculated as the dry biomass per unit surface area (Eq. 4), while biomass productivity ($\text{g.m}^{-2}.\text{day}^{-1}$) was estimated by dividing surface biomass production by the total cultivation period (Eq. 5). In the biomass analysis, the washing step was assumed to remove most bacterial biomass from the *Amphora* biofilm, and any remaining bacterial biomass was considered negligible relative to *Amphora* cells, as attempts at intentional separation could have resulted in *Amphora* biomass loss. This assumption was further supported by fatty acid profile analysis, which showed the absence of branched fatty acids and odd-chain fatty acid such as C17:0, commonly used as bacterial biomarkers (Maltsev and Maltseva, 2021) (see Table 2).

$$\text{Surface biomass production} = \frac{\text{Total dry biomass}}{\text{surface area}} \quad (4)$$

$$\text{Biomass productivity} = \frac{\text{Surface biomass production}}{\text{Total cultivation period}} \quad (5)$$

2.7. Lipid analysis

2.7.1. Total lipid content

Total lipid extraction and quantification were performed as described by Cointet et al. (2019), based on a modified Bligh and Dyer (1959) method. Lyophilized biomass was extracted with 50 mL of dichloromethane/methanol (1:1, v/v) for 24 h. The mixture was filtered (100 mm, 10 μm pleated filter) to remove cell debris. The filtrate was washed with distilled water (50% of its volume) to separate the organic phase, which was then dried over anhydrous Na_2SO_4 , filtered, evaporated under N_2 , and weighed to determine the lipid content. The total lipid rate was expressed as a percentage of the extracted dry biomass (Eq. 6). Surface lipid production (g.m^{-2}) was calculated by normalizing the lipid content to the surface area of the growth substrate (Eq. 7). Lipid productivity ($\text{g.m}^{-2}.\text{day}^{-1}$) was calculated by dividing surface lipid

production in the total duration of the culture period (Eq. 8). Lipid extracts were stored at -20°C in 1 mL of CH_2Cl_2 until fatty acid analysis.

$$\text{Total lipid rate} = \frac{\text{Lipid content}}{\text{Dry biomass weight}} \times 100 \quad (6)$$

$$\text{Surface lipid production} = \frac{\text{Lipid content}}{\text{Surface area}} \quad (7)$$

$$\text{Lipid productivity} = \frac{\text{Surface lipid production}}{\text{Total cultivation period}} \quad (8)$$

2.7.2. Fatty acids profiling

Fatty acid profile analysis was conducted using GC-MS, following the method described by Cointet et al. (2021). Briefly, about 1 mg of crude lipid was transesterified with 500 μL of 3 mol. L^{-1} hydrochloric methanol, 300 μL methanol, and 100 μL chloroform at 80°C for 5 h. After cooling, 500 μL hexane was added and centrifuged (1236 g, 5 min). The hexane phase was dried over Na_2SO_4 and evaporated under N_2 to obtain fatty acids methyl esters (FAMES). For NAP derivatization, dried FAMES were reacted with 500 μL pyrrolidine and 100 μL acetic acid at 85°C for 1 h. After cooling, 4 mL CH_2Cl_2 and 500 μL water were added, shaken, centrifuged (1236 g, 5 min), and the organic phase was dried with Na_2SO_4 and evaporated under N_2 at 40°C . FAMES or NAPs were redissolved in 1 mL CH_2Cl_2 per mg before analysis. The analyses were performed on a GC-MS instrument (GC 8860 coupled with 5977 C MS detector - 70 eV, Agilent Technologies, USA) equipped with an SLB-5TM column (60 m \times 0.25 mm; 0.25 μm , Sigma- Aldrich). The injector and detector temperatures were 250°C and 280°C , respectively. The carrier gas was helium at a flow rate of 1 mL per min. One microliter was injected in splitless mode. The column temperature was set at 170°C for 4 min then increased at 3°C per min to 300°C and hold for 10 min for FAME analyses, and set at 200°C for 5 min, increased by 3°C per min up to 310°C and hold for 10 min for NAP analyses. Chromatogram peaks were evaluated and quantified using OpenChrom Lablicate Edition 1.5.0 (McLafferty). Fatty acid identification was confirmed by comparing mass spectra and retention times with a reference library from previous analyses, available on LipidMaps (<https://www.lipidmaps.org/>).

2.8. Statistical analysis

All experiments were performed in triplicate, and results are expressed as mean \pm standard deviation. The normality of growth, biomass, and lipid data for *Amphora* sp. under axenic, non-axenic, and co-culture conditions in the vertical biofilm PSBR was assessed using the Shapiro-Wilk test. Group comparisons were conducted using one-way ANOVA followed by Tukey's HSD post hoc test for normally distributed data, or the Kruskal-Wallis test followed by Dunn's test for non-normally distributed data. Gompertz growth curves were fitted using the Gompertz function provided in the *theJesus* package in R to build the growth curves of *Amphora* sp. in axenic, non-axenic and co-culture conditions. Multivariate analysis based on biomass and lipid related traits was performed using principal coordinates analysis (PCoA). Differences among culture conditions were assessed using permutational multivariate analysis of variance (PERMANOVA) implemented with the *adonis2()* function in the R package *vegan*, which tests for differences in multivariate centroids among groups in the ordination space. To confirm that significant PERMANOVA results were not driven by differences in within-group dispersion, homogeneity of multivariate dispersions (PERMDISP) was evaluated using functions; *betadisper()* followed by *permutest()* (R package *vegan*). All permutation-based tests used 9999 permutations. Where post hoc pairwise PERMANOVA comparisons were performed, the *pairwise.adonis2()* function from the *pairwiseAdonis* package was used, and *p* values were adjusted using the Benjamini-Hochberg false discovery rate (BH-FDR; *p.adjust.m* = "BH"), with FDR-adjusted *p* values used for inference. Permutation-based vector

fitting was performed using *envfit()* (R package *vegan*) to identify traits significantly correlated with the PCoA axes, indicating variables contributing to group separation. All statistical analyses, visualizations, and tables were generated using RStudio (v4.1.2) and Microsoft Excel 365. Statistical significance was assessed at a 95% confidence level ($p < 0.05$).

3. Results

3.1. Growth assay

NDVI increased significantly in axenic *Amphora* sp. until day 5, in non-axenic *Amphora* sp. until day 7, in the co-culture with *Nitratireductor* sp. until day 2, and in the co-culture with *Sulfitobacter* sp. until day 5 (Tukey's HSD, $p < 0.05$; Fig. 2). After these respective time points, no further significant differences in NDVI were observed within any group. Across groups, significant differences in NDVI were found only on day 0 and day 2, with no differences detected afterward. On both day 0 and day 2, the co-cultures exhibited significantly higher NDVI values compared to both axenic and non-axenic controls (Tukey's HSD, $p < 0.05$). The relative growth rates (μ) of *Amphora* sp. in axenic, non-axenic, and co-cultures with *Nitratireductor* sp. and *Sulfitobacter* sp. in the biofilm PSBR were 0.4 ± 0.1 , 0.3 ± 0.0 , 0.2 ± 0.0 , and 0.2 ± 0.1 day^{-1} , respectively. However, these differences were not statistically significant (Tukey's HSD, $p > 0.05$).

3.2. *Amphora* to bacteria ratio in co-cultures at day 3, 6 and 15

Amphora to bacteria ratios in *Amphora*-*Nitratireductor* and *Amphora*-*Sulfitobacter* co-cultures in the PSBR at days 3, 6, and 15 are shown in Fig. 3. Overall, bacterial populations tended to decline, whereas *Amphora* sp. cell numbers increased from day 3 to day 6, thereafter, both *Amphora* and bacterial populations remained relatively stable. However, the *Amphora*-*Nitratireductor* ratios were 1:1, 3:1, and 2:1 at days 3, 6, and 15, respectively, while the corresponding ratios for the *Amphora*-*Sulfitobacter* co-culture were 1:5, 1:3, and 1:2.

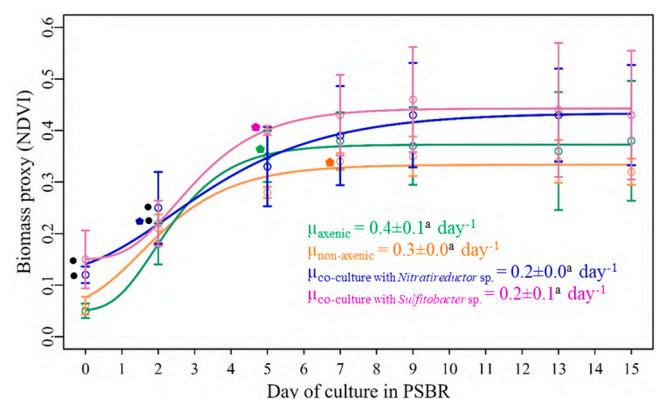


Fig. 2. Average NDVI of axenic *Amphora* sp. (—), non-axenic *Amphora* sp. (—), co-culture of *Amphora* sp. with *Nitratireductor* sp. (—) and co-culture of *Amphora* sp. with *Sulfitobacter* sp. (—) over the 15 days cultivation period in the vertical biofilm PSBR. Error bars represent the standard deviation of the mean NDVI, *n* = 3 biological replicates. The symbol (●) indicates a significant difference from both axenic and non-axenic controls. Unless otherwise specified, no significant differences were observed across other groups on the same day. Colour coded symbol (●) denotes the onset of non-significant changes in NDVI within the respective culture. Superscript letters indicate the significant difference of relative growth rate (μ) across different groups.

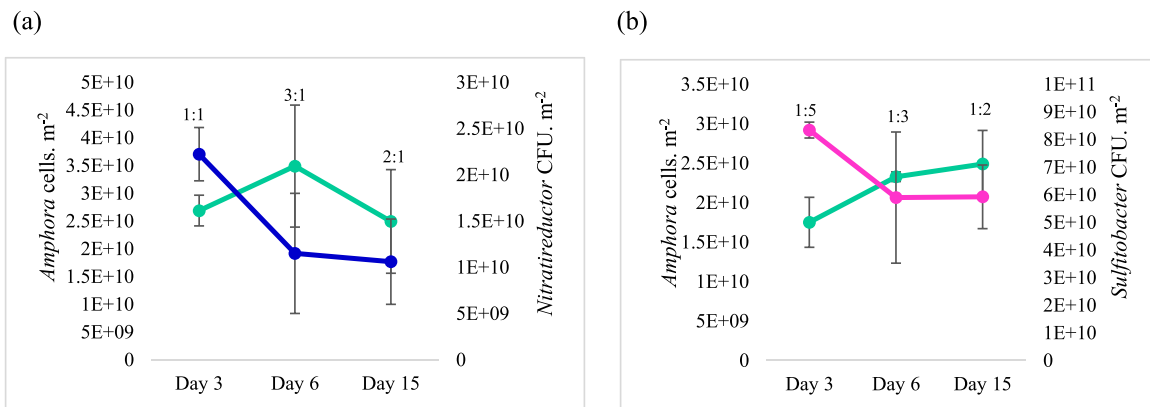


Fig. 3. *Amphora* sp. to bacteria ratio in the vertical biofilm PSBR at day 3, 6 and 15. (a) *Amphora*-*Nitratireductor* co-culture (b) *Amphora*-*Sulfitobacter* co-culture, *Amphora* sp. (—●—), *Nitratireductor* sp. (—●—), *Sulfitobacter* sp. (—●—), Error bars represent the standard deviation of the mean *Amphora* cells per m² or CFUs of bacteria per m², n = 3 biological replicates.

3.3. Photosynthetic efficiency of cultures

The photosynthetic efficiency of all cultures in the PSBR declined gradually over time (Fig. 4). Until day 7, the average Fv/Fm values across all cultures ranged between 0.5 and 0.7, with no significant differences among groups (Tukey's HSD, $p > 0.05$). After day 9, Fv/Fm in non-axenic *Amphora* sp. dropped below 0.5 but remained statistically similar to axenic *Amphora* sp. culture on days 9, 13, and 15. Both co-cultures also showed Fv/Fm values below 0.5 from day 9 onward.

3.4. Surface biomass production and productivity

The highest surface biomass production was observed in *Amphora* sp. co-cultured with *Nitratireductor* sp. on days 3 and 6, reaching 2.54 ± 0.39 g.m⁻² and 7.27 ± 1.31 g.m⁻², respectively (Fig. 5). This was significantly higher than the non-axenic *Amphora* sp. (Tukey's HSD, $p < 0.05$) but not significantly different from the axenic *Amphora* sp. culture and the co-culture with *Sulfitobacter* sp. By day 15, no significant differences in surface biomass were observed among the groups (Tukey's HSD, $p > 0.05$). The final biomass values were 6.06 ± 0.74 g.m⁻² for the axenic culture, 4.28 ± 0.19 g.m⁻² for the non-axenic culture, 6.45 ± 1.50 g.m⁻² for the *Nitratireductor* sp. co-culture, and 7.21 ± 3.02 g.m⁻² for the *Sulfitobacter* sp. co-culture. Although surface biomass production of the axenic culture tended to be higher than that of the

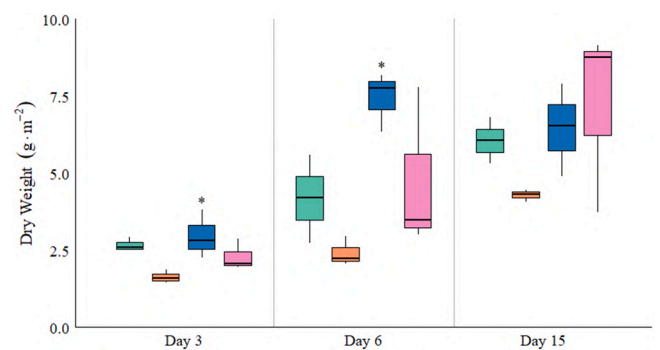


Fig. 5. The surface biomass production (g.m⁻²) of axenic *Amphora* sp. (—●—), non-axenic *Amphora* sp. (—●—), co-culture of *Amphora* sp. with *Nitratireductor* sp. (—●—) and co-culture of *Amphora* sp. with *Sulfitobacter* sp. (—●—) in the vertical biofilm PSBR at days 3, 6 and 15. Error bars represent the standard deviation of the mean surface biomass production. n = 3 biological replicates. The symbol (*) indicates a significant difference from the non-axenic control. Unless otherwise specified, no significant differences were observed across other groups on the same day.

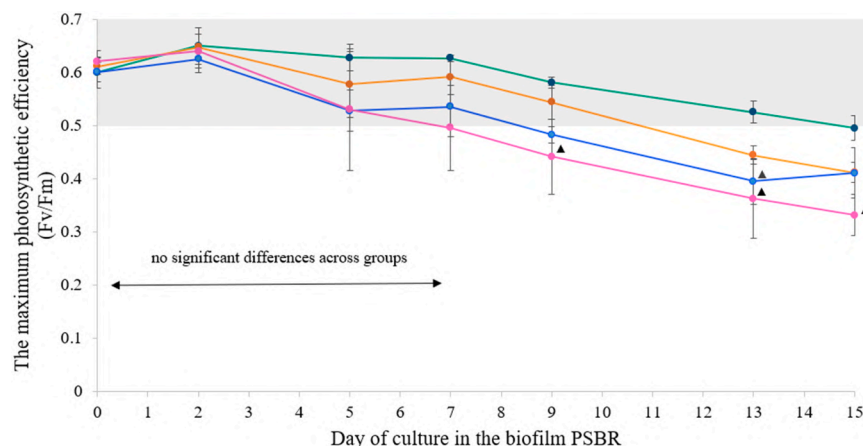


Fig. 4. The average maximum photosynthetic efficiency (Fv/Fm) of axenic *Amphora* sp. (—●—), non-axenic *Amphora* sp. (—●—), co-culture of *Amphora* sp. with *Nitratireductor* sp. (—●—) and co-culture of *Amphora* sp. with *Sulfitobacter* sp. (—●—) in the vertical biofilm PSBR over the 15 days cultivation period. Error bars represent the standard deviation of the mean Fv/Fm. n = 3 biological replicates. The symbol (▲) indicates a significant difference from the axenic control. Unless otherwise specified, no significant differences were observed across other groups on the same day. The grey-coloured area represents the typical threshold range of Fv/Fm (0.5–0.7) for diatoms, indicating non-physiological stress.

non-axenic culture on all three harvesting days, the difference was not statistically significant (Tukey's HSD, $p > 0.05$).

Regarding biomass productivity, the axenic *Amphora* sp. culture and both co-cultures consistently outperformed the non-axenic culture on days 3 and 6 (Table 1). The highest biomass productivities were recorded in the co-culture with *Nitratireductor* sp. on days 3 and 6, reaching 0.99 ± 0.26 and 1.24 ± 0.16 g.m⁻².day⁻¹, respectively. On day 15, the co-culture with *Sulfitobacter* sp. showed the highest biomass productivity (0.48 ± 0.20 g.m⁻².day⁻¹). However, biomass productivity in both co-cultures did not differ significantly from the axenic *Amphora* sp. (Tukey's HSD, $p > 0.05$) at all three harvesting days.

3.5. Surface lipid production and productivity

On day 3, *Amphora* sp. co-cultured with *Sulfitobacter* sp. showed significantly higher surface lipid production (1.51 ± 0.31 g.m⁻², Tukey's HSD, $p < 0.05$) than both controls and the co-culture with *Nitratireductor* sp. (Fig. 6). A similar pattern was observed in lipid productivity (Table 1), with the *Sulfitobacter* co-culture (0.50 ± 0.10 g.m⁻².day⁻¹) being significantly higher than the controls and *Amphora-Nitratireductor* co-culture. On day 6, no significant differences in surface lipid production were observed among controls and co-cultures (Tukey's HSD, $p > 0.05$). However, the non-axenic *Amphora* sp. displayed significantly lower lipid productivity (0.08 ± 0.01 g.m⁻².day⁻¹) than both co-cultures (Tukey's HSD, $p < 0.05$), although it was not significantly different from the axenic condition. By day 15, non-axenic *Amphora* sp. exhibited significantly higher surface lipid production (1.80 ± 0.21 g.m⁻²) than both co-cultures (Tukey's HSD, $p < 0.05$), though not significantly different from the axenic condition (1.28 ± 0.16 g.m⁻²). Likewise, lipid productivity of non-axenic *Amphora* (0.12 ± 0.01 g.m⁻².day⁻¹) was also significantly higher (Tukey's HSD, $p < 0.05$) than that of the co-cultures (Tukey's HSD, $p < 0.05$), with no difference from the axenic condition (Tukey's HSD, $p > 0.05$).

3.6. Relative lipid content to biomass

Amphora sp. co-cultured with *Sulfitobacter* sp. exhibited the significantly highest lipid content relative to its dry biomass weight (DW) ($67.03 \pm 17.80\%$) than those of the controls and the co-culture with *Nitratireductor* sp. (Tukey's HSD, $p < 0.05$, Table 1). By day 6, lipid content (% DW) did not differ significantly among cultures (Tukey's HSD, $p > 0.05$). On day 15, the non-axenic *Amphora* sp. exhibited a significantly higher lipid content ($42.19 \pm 2.29\%$) compared to the axenic culture and both co-cultures (Tukey's HSD, $p < 0.05$).

3.7. Fatty acids composition

In total, seven saturated fatty acids (SFAs), three monounsaturated fatty acids (MUFAs), and six polyunsaturated fatty acids (PUFAs) were identified in *Amphora* sp. under axenic, non-axenic, and co-culture conditions (Table 2). The identified SFAs included myristic acid

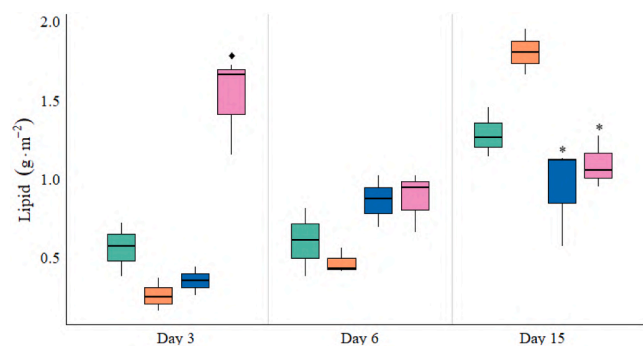


Fig. 6. The surface lipid production (g.m⁻²) of axenic *Amphora* sp. (■), non-axenic *Amphora* sp. (□), co-culture of *Amphora* sp. with *Nitratireductor* sp. (■) and co-culture of *Amphora* sp. with *Sulfitobacter* sp. (■) in the vertical biofilm PSBR at days 3, 6 and 15. Error bars represent the standard deviation of the mean surface lipid production. n = 3 biological replicates. The symbol ◆ indicates a significant difference from both controls (axenic and non-axenic) and the other co-culture, while * indicates a significant difference from the non-axenic control. Unless otherwise specified, no significant differences were observed across other groups on the same day.

(14:0), pentadecanoic acid (15:0), palmitic acid (16:0), stearic acid (18:0), arachidic acid (20:0), behenic acid (22:0), and lignoceric acid (24:0). However, arachidic acid, behenic acid, and lignoceric acid were not detected in any of the co-culture samples at any of the harvesting time points. Among the SFAs, palmitic acid (16:0) was the most abundant across all culture conditions and harvesting days, accounting for 20–55% of the total fatty acid content. Notably, stearic acid (18:0) content was significantly higher in non-axenic *Amphora* sp. on day 3 ($21.45 \pm 0.93\%$) compared to the axenic and co-culture conditions (Tukey's HSD, $p < 0.05$). On all other days, stearic acid levels remained below 15% in all cultures. On days 3, 6 and 15, no significant differences in total SFA content were observed among the control and co-culture conditions. However, the highest SFA content on day 3 and 6 was recorded in non-axenic *Amphora* sp. reaching approximately 60%–67%, while on day 15, it was observed in the co-culture with *Nitratireductor* sp. ($48.57 \pm 3.66\%$). The most abundant MUFAs was palmitoleic acid (16:1), which was present in all cultures across all harvesting days, accounting for 19–58% of the total fatty acid content. Oleic acid (9–18:1) levels in *Amphora* sp. did not differ significantly among cultures at any harvesting day, although the co-culture with *Nitratireductor* sp. consistently tended to exhibit higher oleic acid content. In contrast, 11-octadecenoic acid (11–18:1) was detected exclusively in co-cultures at all harvesting days, with levels below 1.5%. Regarding total MUFAs content, a significantly lower MUFAs percentage was observed in non-axenic *Amphora* sp. on day 3 ($25.41 \pm 3.41\%$) (Tukey's HSD, $p < 0.05$). On day 6, the co-culture with *Nitratireductor* sp. showed a significantly higher MUFAs content ($51.29 \pm 2.35\%$), although it was

Table 1

Lipid % DW, lipid productivity (g.m⁻².day⁻¹) and biomass productivity (g.m⁻².day⁻¹) of *Amphora* sp. in axenic, non-axenic and co-culture conditions with *Nitratireductor* sp. (CC1) and *Sulfitobacter* sp. (CC2) at day 3, 6, and 15 in the vertical biofilm PSBR.

	Lipid % DW				Lipid productivity (g.m ⁻² .day ⁻¹)				Biomass productivity (g.m ⁻² .day ⁻¹)			
	Axenic	Non-axenic	CC1	CC2	Axenic	Non-axenic	CC1	CC2	Axenic	Non-axenic	CC1	CC2
Day 3	20.62 ± 5.22	16.58 ± 8.78	11.79 ± 0.51	67.03 ± 17.80◆	0.19 ± 0.06	0.09 ± 0.04	0.12 ± 0.03	0.50 ± 0.10◆	0.89 ± 0.08	0.55 ± 0.07	0.99 ± 0.26*	0.76 ± 0.16
Day 6	14.73 ± 4.23	20.04 ± 6.54	11.69 ± 2.55	23.16 ± 13.13	0.10 ± 0.04	0.08 ± 0.01	0.14 ± 0.03*	0.15 ± 0.03*	0.70 ± 0.24	0.40 ± 0.08	1.24 ± 0.16*	0.79 ± 0.44
Day 15	21.17 ± 0.28*	42.19 ± 2.29	15.77 ± 7.92*	17.68 ± 9.25*	0.09 ± 0.01	0.12 ± 0.01	0.06 ± 0.02*	0.07 ± 0.01*	0.40 ± 0.05	0.29 ± 0.01	0.43 ± 0.10	0.48 ± 0.20

The symbols ◆ and * indicate a significant difference from both controls (axenic and non-axenic) and the other co-culture, and from the non-axenic control, respectively. Unless otherwise specified, no significant differences were observed among the other groups on the same day.

Table 2

Fatty acid composition of *Amphora* sp. under axenic, non-axenic, and co-culture conditions with *Nitratireductor* sp. (CC1) and *Sulfitobacter* sp. (CC2) on days 3, 6, and 15, cultivated in the vertical biofilm PSBR.

Fatty acid	Day of the culture in the PSBR											
	Day 3				Day 6				Day 15			
	Axenic	Non-axenic	CC1	CC2	Axenic	Non-axenic	CC1	CC2	Axenic	Non-axenic	CC1	CC2
Saturated fatty acids (SFA)												
14:0	9.19 ± 0.72	ND	1.57 ± 1.06 [▲]	0.96 ± 0.93 [▲]	3.05 ± 0.36	ND	2.57 ± 0.68	1.02 ± 0.80 [▲]	3.36 ± 2.91	8.37 ± 7.25	1.35 ± 0.96	3.34 ± 2.16
15:0	ND	0.17 ± 0.16	0.36 ± 0.24	0.33 ± 0.29	ND	ND	0.97 ± 0.30	0.48 ± 0.25	0.22 ± 0.38	0.66 ± 0.60	1.12 ± 0.56	2.45 ± 1.83
16:0	39.69 ± 1.81	33.99 ± 1.73	43.33 ± 5.12	45.01 ± 5.39 [*]	31.48 ± 0.61 ^a	45.43 ± 8.25 ^b	40.47 ± 3.08	45.46 ± 2.50 [▲]	37.20 ± 6.75	28.32 ± 7.24	42.50 ± 2.60 [*]	34.65 ± 2.12
18:0	2.94 ± 1.76 [*]	21.45 ± 0.93	3.30 ± 1.89 [*]	2.30 ± 0.36 [*]	6.99 ± 2.45	9.99 ± 4.29	1.84 ± 0.44 [*]	3.36 ± 0.52	3.12 ± 1.66	5.18 ± 2.88	3.61 ± 2.48	1.28 ± 0.21
20:0	0.04 ± 0.04 ^a	0.75 ± 0.28 ^b	ND	ND	0.29 ± 0.05	0.24 ± 0.07	ND	ND	0.06 ± 0.06	0.12 ± 0.10	ND	ND
22:0	ND	0.69 ± 0.64	ND	ND	0.28 ± 0.30	0.25 ± 0.07	ND	ND	0.02 ± 0.04	0.09 ± 0.10	ND	ND
24:0	0.11 ± 0.03 ^a	1.33 ± 0.62 ^b	ND	ND	0.75 ± 0.25	0.72 ± 0.37	ND	ND	0.19 ± 0.10	0.39 ± 0.20	ND	ND
Σ SFA	51.97 ± 0.69	59.26 ± 1.07	48.55 ± 4.34	48.59 ± 4.36	43.18 ± 1.95	56.89 ± 10.24	45.85 ± 1.69	50.31 ± 3.24	44.19 ± 5.86	43.18 ± 3.39	48.57 ± 3.66	41.73 ± 1.76
Monounsaturated fatty acids (MUFA)												
9–16:1	40.86 ± 1.65 ^a	20.81 ± 1.08 ^b	32.87 ± 9.43	43.94 ± 0.48 [*]	32.36 ± 1.00	26.40 ± 3.69	39.83 ± 3.07 [*]	39.01 ± 2.69 [*]	37.69 ± 2.59	47.03 ± 10.20	38.80 ± 7.49	44.73 ± 2.89
9–18:1	1.43 ± 1.04	4.60 ± 2.35	15.80 ± 12.34	1.64 ± 1.53	2.97 ± 0.67	3.77 ± 1.16	10.92 ± 5.29	4.17 ± 3.21	1.57 ± 0.46	1.38 ± 0.10	8.11 ± 6.52	2.43 ± 0.51
11–18:1	ND	ND	0.82 ± 0.46	0.53 ± 0.13	ND	ND	0.54 ± 0.13	1.02 ± 0.14	ND	ND	0.55 ± 0.33	0.77 ± 0.20
Σ MUFA	42.29 ± 1.10[*]	25.41 ± 3.41	49.49 ± 3.70[*]	46.11 ± 2.01[*]	35.33 ± 1.37	30.17 ± 2.65	51.29 ± 2.35[*]	44.19 ± 1.52	39.26 ± 2.14	48.41 ± 10.29	47.47 ± 4.45	47.94 ± 3.09
Polyunsaturated fatty acids (PUFA)												
6,9,12–16:3	0.28 ± 0.22	0.07 ± 0.08	ND	ND	0.59 ± 0.12	ND	ND	ND	0.25 ± 0.21	0.09 ± 0.09	ND	0.66 ± 0.58
6,9,12–18:3	0.11 ± 0.03 ^a	0.43 ± 0.05 ^b	0.24 ± 0.13	0.44 ± 0.17 [▲]	0.44 ± 0.12	0.18 ± 0.13	0.26 ± 0.08	0.65 ± 0.26 [*]	0.40 ± 0.28	0.25 ± 0.16	0.29 ± 0.12	0.66 ± 0.26
6,9,12,15–18:4	0.89 ± 0.13 ^a	2.38 ± 0.68 ^b	ND	ND	3.04 ± 0.41	1.70 ± 1.44	ND	ND	2.19 ± 1.11	1.48 ± 1.03	ND	ND
9,12–18:2	0.56 ± 0.06 [*]	1.91 ± 0.38	0.31 ± 0.32 [*]	0.45 ± 0.22 [*]	1.79 ± 0.16	1.33 ± 0.60	0.44 ± 0.16 [▲]	0.82 ± 0.27 [▲]	1.90 ± 0.88	1.17 ± 0.45	0.53 ± 0.38	0.79 ± 0.35
5,8,11,14–20:4	0.07 ± 0.03 ^a	0.47 ± 0.06 ^b	ND	ND	0.60 ± 0.19	0.20 ± 0.25	ND	ND	0.57 ± 0.42	0.09 ± 0.15	ND	ND
5,8,11,14,17–20:5	3.66 ± 0.23	9.36 ± 3.94	0.92 ± 0.97 [*]	4.41 ± 2.31	13.98 ± 2.44	9.35 ± 10.38	1.64 ± 1.12 [▲]	4.02 ± 2.08 [▲]	10.91 ± 4.51	5.05 ± 6.41	2.23 ± 1.19	8.22 ± 0.63
ω-3 FAs	4.55 ± 0.35[*]	11.74 ± 4.57	0.92 ± 0.97[*]	4.41 ± 2.31[*]	17.02 ± 2.54	11.04 ± 11.82	1.64 ± 1.12	4.02 ± 2.08	13.10 ± 5.60	6.53 ± 7.19	2.23 ± 1.19	8.22 ± 0.63
ω-6 FAs	1.03 ± 0.33[*]	2.89 ± 0.35	0.55 ± 0.44[*]	0.88 ± 0.39[*]	3.42 ± 0.38	1.71 ± 0.98	0.70 ± 0.20[▲]	1.47 ± 0.53	3.12 ± 1.78	1.60 ± 0.58	0.82 ± 0.49	2.10 ± 1.17
Σ PUFA	5.57 ± 0.68[*]	14.62 ± 4.27	1.47 ± 1.41[*]	5.29 ± 2.66[*]	20.44 ± 2.31	12.75 ± 12.77	2.34 ± 1.29[▲]	5.50 ± 2.59[▲]	16.22 ± 7.32	8.13 ± 7.70	3.05 ± 1.69	10.33 ± 1.52

The symbols ▲ and * indicate a significant difference from axenic *Amphora* sp. and from the non-axenic *Amphora* sp., respectively. Superscript letters indicate the significant differences between axenic and non-axenic *Amphora* sp. cultures. Unless otherwise specified, no significant differences were observed among the other groups on the same day. 14:0 – Myristic acid, 15:0 – Pentadecanoic acid, 16:0 – Palmitic acid, 18:0 – Stearic acid, 20:0 – Arachidic acid, 22:0 – Behenic acid, 24:0 – Lignoceric acid, 9–16:1 – Palmitoleic acid, 9–18:1 – Oleic acid, 11–18:1 – 11-Octadecenoic acid, 6,9,12–16:3 – Hexadecatrienoic acid, 6,9,12–18:3 – γ-Linolenic acid, 6,9,12,15–18:4 – Stearidonic acid, 9,12–18:2 – Linoleic acid, 5,8,11,14–20:4 – Arachidonic acid, 5,8,11,14,17–20:5 – Eicosapentaenoic acid, ω-3 fatty acids (FAs)– 6,9,12–16:3 and 5,8,11,14,17–20:5, ω-6 fatty acids (FAs)– 6,9,12–18:3, 6,9,12,15–18:4, 9,12–18:2, and 5,8,11,14–20:4

significantly different only from the non-axenic *Amphora* sp. condition. By day 15, no significant differences in MUFAs content were observed among cultures, with values ranging from 37% to 60%. *Amphora* sp. contained a considerably lower amount of PUFAs compared to SFAs and MUFAs. A total of four ω-6 PUFAs (γ-linolenic acid (6,9,12–18:3), stearidonic acid (6,9,12,15–18:4), linoleic acid (9,12–18:2), and arachidonic acid (5,8,11,14–20:4)) and two ω-3 PUFAs (hexadecatrienoic acid (6,9,12–16:3) and eicosapentaenoic acid (EPA; 5,8,11,14,17–20:5)) were identified in *Amphora* sp. However, stearidonic acid and arachidonic acid were not found in both co-cultures throughout the culture period. Among all PUFAs, EPA was highest in

non-axenic *Amphora* sp. on day 3 (9.36 ± 3.94%), but it didn't significantly different from axenic control and *Amphora-Sulfitobacter* co-culture. On days 6 and 15, the highest levels were consistently recorded in axenic *Amphora* sp., with values of 13.98 ± 2.44% and 10.91 ± 4.51%, respectively, while the difference was significant only on day 6 compared to both co-cultures. Overall, non-axenic *Amphora* sp. exhibited significantly higher total PUFA on day 3 compared to all other cultures, while PUFA content largely mirrored the differences in EPA observed across all conditions on days 6 and 15.

3.8. Nutrients

The concentrations of all major nutrients in the culture medium, DIN, DIP, DSI, and ammonium decreased over time (Fig. 7). Notably, the consumption of DIN by *Amphora* sp. in co-culture with *Nitratireductor* sp. remained unchanged until day 6, with concentrations remaining around 888 $\mu\text{mol.L}^{-1}$. In contrast, both the axenic and non-axenic controls, along with the co-culture with *Sulfitobacter* sp., exhibited a gradual decrease in DIN levels over the same period. Meanwhile, DIP, DSI and ammonium levels declined sharply across all cultures between day 0 and day 6. In particular, DIP dropped from approximately 36 $\mu\text{mol.L}^{-1}$ to below 2 $\mu\text{mol.L}^{-1}$, DSI from 106 $\mu\text{mol.L}^{-1}$ to below 50 $\mu\text{mol.L}^{-1}$, and ammonium from 555 $\mu\text{mol.L}^{-1}$ to below 60 $\mu\text{mol.L}^{-1}$. By day 15, axenic *Amphora* sp. and both co-cultures had consumed nearly 50% of the total DIN, along with approximately 98% of DIP, 85% of DSI and 99% of ammonium.

3.9. Overall co-culture effects on *Amphora* sp. biomass-lipid profiles

The overall impact of bacterial co-culturing on *Amphora* sp. biomass and lipid traits is shown in Fig. 8. PERMANOVA revealed a significant separation among culture conditions in the ordination space ($p < 0.05$), while the non-significant PERMDISP result confirmed that this separation was not driven by differences in within-group dispersion. Most biomass and lipid related traits, with the exception of biomass productivity, were significantly correlated with the PCoA axes. Notably, the *Amphora-Sulfitobacter* co-culture at day 3 cluster distinctly to the right along PCoA1, indicating higher lipid productivity and lipid % DW while the day 6 group overlaps with the axenic and *Amphora-Nitratireductor* groups but trends toward higher lipid production. The *Amphora-Sulfitobacter* group at day 15 shifts upward along PCoA2, consistent with additional biomass gains compared to other days. *Nitratireductor* co-cultures at all three harvest points largely overlap and plot higher on PCoA2 with moderate PCoA1, reflecting a biomass advantage with only modest lipid enrichment. Axenic cultures remain near the origin, exhibiting intermediate lipid and biomass values. Non-axenic cultures at day 3 and day 6 lie on the negative PCoA1 axis, highlighting lower biomass with an SFA and PUFA leaning profiles, whereas the day 15 group shifts toward positive PCoA2, indicating increasing lipid content with higher MUFA levels.

4. Discussion

Binary co-cultivation of bacteria and benthic diatom biofilms in

efficient biofilm cultivation systems such as PSBRs presents an innovative approach to enhancing both biomass and lipid production in microalgal biofilms. Compared to complex multispecies consortia, these simplified co-culture systems allow for more controlled investigations of microalgae-bacteria interactions, offering clearer mechanistic insights and scalable strategies for industrial bioprocess optimization (Rasheed et al., 2023; Tong et al., 2023). In our study, growth kinetics of *Amphora* sp. in the laboratory scale vertical biofilm PSBR over a 15-day batch culture revealed clear physiological shifts from the exponential to stationary phase under bacterial influence, while the absence of a distinct lag phase in any culture was likely due to the 4-day pre-incubation period in microwell plates. Notably, *Amphora* sp. in co-culture with *Nitratireductor* sp. entered the stationary phase by day 2 earlier than all other cultures, likely due to accelerated early growth and biofilm development, as reflected by significantly higher NDVI values during the first two days, suggesting a beneficial interaction. This early physiological shift was more likely triggered by spatial constraints arising from the rapid growth of *Amphora* in co-culture with *Nitratireductor*, as no nutrient depletion was observed until day 6. The delayed onset of the stationary phase in non-axenic *Amphora* sp. (day 7), compared with axenic (day 5) and co-culture conditions, may be attributed to the complementary roles of its natural microbiota in supporting algal growth and mitigating potential negative effects, such as nutrient and space competition arising from multiple bacterial interactions (Cho et al., 2015). These microbial communities likely support sustained growth through nutrient recycling (González-González and De-Bashan, 2021), exchange of growth-promoting metabolites such as indole-3-acetic acid (IAA) (Lépinay et al., 2018; Chorzyczewski et al., 2021; Sittmann et al., 2021), or by mitigating stress that may arise from antagonistic interactions (Fuentes et al., 2016). Considering the maximum photosynthetic efficiency of *Amphora* sp. under each culture condition, axenic *Amphora* sp. exhibited healthy metabolic activity and minimal physiological stress, maintaining values within the optimal range of 0.5–0.7 throughout the cultivation period (Arnaldo et al., 2024a). In contrast, from day 9 onward, *Amphora* sp. in the non-axenic and co-culture conditions showed a decline in photosynthetic efficiency, indicating the onset of physiological stress. This decline may be attributed to spatial constraints (Zeng et al., 2023), light limitation due to increased biofilm density (Wang et al., 2021), nutrient deficiency (Arnaldo et al., 2024), or biotic stress resulting from bacteria during the stationary phase, when microalgal metabolic activity naturally declines (Steinrücken et al., 2023). Furthermore, the observed non-significant differences in relative growth rates among the controls and co-cultures may be attributed to the significantly higher NDVI values at day 0 in

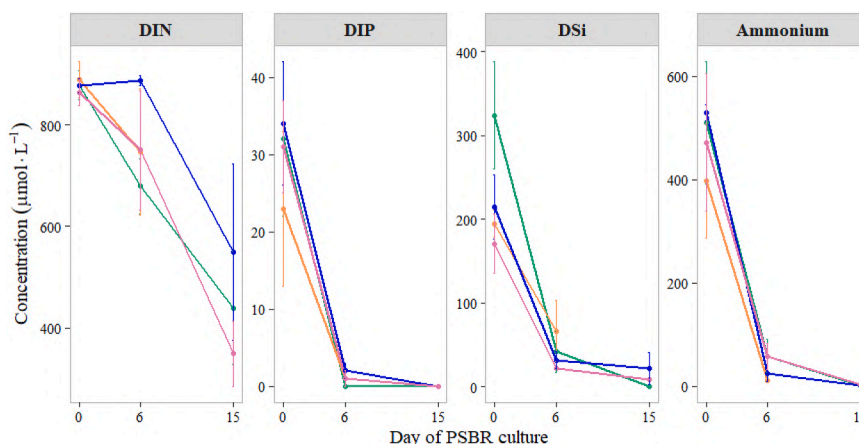


Fig. 7. Average nutrient availability in the culture medium of axenic *Amphora* sp. (—●—), non-axenic *Amphora* sp. (—■—), co-culture of *Amphora* sp. with *Nitratireductor* sp. (—◆—) and co-culture of *Amphora* sp. with *Sulfitobacter* sp. (—▲—) in the vertical biofilm PSBR at day 0, 6 and 15 (excluding data for the 15-day non-axenic *Amphora* sp. cultures; see Section 2.5). Error bars represent the standard deviation of the mean DIN, DIP, DSI or ammonium at each respective time point, n = 3.

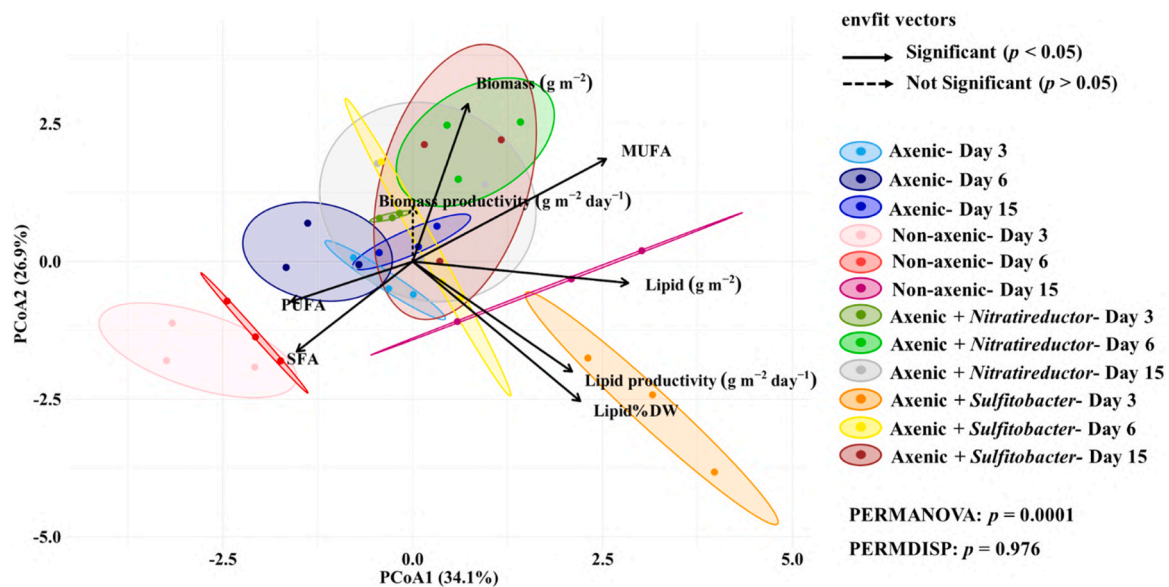


Fig. 8. PCoA of biomass and lipid-related traits of *Amphora* sp. grown in the vertical biofilm PSBR under four conditions: axenic, non-axenic, axenic + *Nitratireductor* sp., and axenic + *Sulfitobacter* sp. Cultures were sampled on days 3, 6, and 15. $n = 3$ biological replicates. Variables included lipid content ($\text{g}\cdot\text{m}^{-2}$), lipid % of dry weight, lipid productivity ($\text{g}\cdot\text{m}^{-2}\cdot\text{day}^{-1}$), biomass ($\text{g}\cdot\text{m}^{-2}$), biomass productivity ($\text{g}\cdot\text{m}^{-2}\cdot\text{day}^{-1}$), and fatty acid classes (SFA, MUFA and PUFA). Solid arrows represent variables significantly correlated with the PCoA axes (envfit, $p < 0.05$), whereas dashed arrows indicate non-significant correlations ($p > 0.05$). PERMANOVA p -value < 0.05 indicates significant separation among groups, while a non-significant PERMDISP p -value confirms that this significance is not driven by within-group variance.

the co-cultures, which could have reduced variability in the calculated growth rates due to a shorter exponential growth phase. Likewise, comparable growth rates for the genus *Amphora* have been reported across various culture conditions and modes, ranging from 0.2 to 0.5 day^{-1} in both lab scale photobioreactors and outdoor systems (La Peña, 2007; Indrayani et al., 2019; Cointet et al., 2019; Arnaldo et al., 2024a).

Surface biomass production and biomass productivity of axenic *Amphora* sp. and both co-cultures outperformed those of non-axenic *Amphora* sp. across all harvesting days. This trend may be attributed to the absence of harmful bacteria in the axenic culture, which likely reduced competition or the production of inhibitory metabolites, and to the presence of beneficial bacteria in the co-cultures that supported *Amphora* sp. growth (Cho et al., 2015). Notably, the highest surface biomass and biomass productivity were recorded for *Amphora* sp. co-cultured with *Nitratireductor* sp. on day 3 ($2.54 \pm 0.39 \text{ g}\cdot\text{m}^{-2}$; $0.99 \pm 0.26 \text{ g}\cdot\text{m}^{-2}\cdot\text{day}^{-1}$) and day 6 ($7.27 \pm 1.31 \text{ g}\cdot\text{m}^{-2}$; $1.24 \pm 0.16 \text{ g}\cdot\text{m}^{-2}\cdot\text{day}^{-1}$) in the PSBR, followed by a declining trend by day 15. Among all cultures, this was the only one that showed no utilization of inorganic nitrogen in the culture medium until day 6, after which nitrogen consumption began. Further, the *Nitratireductor* population also shifted distinctly over time, from the initial inoculation ratio of *Amphora* to *Nitratireductor* (10:1) to 1:1 by day 3, indicating rapid bacterial proliferation, before declining to 3:1 by day 6 and 2:1 by day 15. Taken together, the absence of detectable nitrogen drawdown in the *Amphora*-*Nitratireductor* co-culture during the early culture period in the PSBR highlights altered nitrogen dynamics within the biofilm, which could potentially be linked to the higher *Nitratireductor* population at the beginning of the co-culture. While the genus *Nitratireductor* has been reported to harbour functional traits associated with nitrogen fixation (diazotrophy) (Ouyabe et al., 2019; Llamas et al., 2023), the N_2 -fixing capacity of *Nitratireductor* sp. should be further tested in future studies, both with and without external nitrogen, as shown by Chandola et al. (2025), where *Phaeodactylum tricornutum* can survive in the absence of external nitrogen through associations with N_2 -fixing bacteria. Alternatively, the observed increase in biomass may also result from metabolic interactions involving small peptides (e.g., diketopiperazines), phytohormones (e.g., IAA, cytokinins, and gibberellins), or other

metabolites (Wang et al., 2015; Lépinay et al., 2018; Chorazyczewski et al., 2021; Sittmann et al., 2021). The co-culture of *Amphora* sp. with *Sulfitobacter* sp. also showed the potential to reach a maximum surface biomass production of approximately $9 \text{ g}\cdot\text{m}^{-2}$ by day 15. These favourable biomass results under co-culture conditions in batch culture mode suggest earlier biomass harvests compared to previous monoalgal studies in PSBRs, where marine algae like *Isochrysis* sp., *Tetraselmis suecica*, *Phaeodactylum tricornutum*, and *Nannochloropsis* sp. dry biomass yielded 10–15 $\text{g}\cdot\text{m}^{-2}$ only after 25 days, with biomass productivities of 0.6–1.8 $\text{g}\cdot\text{m}^{-2}\cdot\text{day}^{-1}$. In addition, co-cultivation with bacteria may reduce the need for external nutrient inputs, such as inorganic nitrogen, thereby supporting lower overall production costs. However, some studies report exceptionally high surface dry biomass productivity in indoor PSBR systems, with green algae such as *Scenedesmus obliquus* reaching an average of $80 \text{ g}\cdot\text{m}^{-2}\cdot\text{day}^{-1}$ (Liu et al., 2013) and *Halochlorella rubescens* achieving approximately $31 \text{ g}\cdot\text{m}^{-2}\cdot\text{day}^{-1}$ (Schultze et al., 2015). These variabilities arise from factors such as design configuration, culture mode (batch, continuous), algal species, culture medium composition, temperature, light intensity and light utilization efficiency as well as the materials used for attachment (Gross et al., 2013; Arnaldo et al., 2024a and b). However, all our cultures exhibited continuous biomass accumulation until the end of cultivation period, but there was a noticeable reduction in biomass productivity over time, indicating entry into the stationary phase where cell division ceases, similar to the observation by Liu et al. (2013). In agreement with our findings, bacterial strains from the genera *Nitratireductor* and *Sulfitobacter* have been shown to enhance microalgal biomass in suspension cultures. For example, *Nitratireductor* sp. has previously been shown to significantly enhance the biomass of *Nannochloropsis oceanica* in co-culture (Liu et al., 2020) while *Sulfitobacter* sp. promoted the growth of the diatom *Pseudo-nitzschia multiseries* through the production and release of IAA, a growth-promoting phytohormone that stimulates cell division (Amin et al., 2015).

The exceptionally high surface lipid production ($1.51 \pm 0.31 \text{ g}\cdot\text{m}^{-2}$), lipid productivity ($0.50 \pm 0.10 \text{ g}\cdot\text{m}^{-2}\cdot\text{day}^{-1}$), and lipid content ($67.03 \pm 17.80\%$ DW) observed in the *Amphora*-*Sulfitobacter* co-culture at day 3, followed by a decline in all parameters over time, suggest a link

between the high bacterial density at day 3 (1 cell.m⁻² of *Amphora* sp.–5 CFU.m⁻² of *Sulfitobacter* sp.) and its subsequent decrease. Under non-limiting nutrient conditions and favourable physiological status of *Amphora* (Fv/Fm) at day 3, this early increase in lipid production is more likely related to concentration-dependent bacterial metabolites, as described by Ji et al. (2018) and Sittmann et al. (2021), and warrants further investigation. In controls, non-axenic *Amphora* sp. maintained relatively stable lipid productivity across all harvesting days. This sustained performance may be attributed to the presence of diverse bacterial populations, which likely played complementary roles in stabilizing culture conditions, facilitating nutrient remineralization, and delaying metabolic decline. Such interactions may have helped prolong the stationary phase, potentially explaining the nearly twofold increase in lipid content (42% DW) observed by day 15 compared to day 6. The lipid content (% DW) and lipid productivity of this strain are consistent with previous studies using the same strain in Erlenmeyer flasks (Cointet et al., 2019), in an airlift photobioreactor (Cointet et al., 2021), and in a 7-day culture within the same PSBR system (Arnaldo et al., 2024a), except for the *Amphora* sp. co-culture with *Sulfitobacter* sp. on day 3, which showed noticeably higher lipid accumulation. Although variations in lipid production were observed across the co-culture conditions, the fatty acid composition of *Amphora* sp. remained largely stable over time and comparable to that of the control cultures. Conversely, several studies have reported shifts in microalgal fatty acid profiles under biotic stress (Cho et al., 2015; Molina-Cárdenas et al., 2020). In general, *Amphora* sp. is rich in palmitic acid (16:0) and palmitoleic acid (16:1), which together can account for nearly 90% of its total fatty acids, while the PUFA content remains comparatively low. The fatty acid profile of *Amphora* sp., rich in palmitic and palmitoleic acids, supports its use in pharmaceutical, nutraceutical, and cosmetic products due to their emollient, moisturizing, and structural functions (Cointet et al., 2019, 2021). Additionally, its high MUFAs and low PUFAs content is favourable for biodiesel quality, providing a good balance of oxidative stability and cold flow properties (Molina-Cárdenas et al., 2020; Cointet et al., 2021). However, the rigid silica frustule of diatoms, comprising up to 50–60% of their dry biomass, can hinder solvent penetration and thus complicate lipid extraction (Pasquet et al., 2011; Bayu et al., 2020), although this was not the focus of our study. In a biorefinery context, the high siliceous content of diatom biomass reduces its calorific value and increases ash production, which can lead to biochar formation, catalyst deactivation, corrosion, and even equipment failure due to the abrasive nature of silica (Hess et al., 2019). These constraints underscore the importance of implementing appropriate pretreatment strategies such as water or alkaline washing, ultrasonication, or microwave-assisted disruption to enable the efficient recovery of targeted metabolites from diatoms (Pasquet et al., 2011; Hess et al., 2019).

Overall, our study provides fundamental insights into the bacterial influence on the growth, biomass, and lipid production of a biofilm forming marine benthic diatom within a lab scale vertical biofilm PSBR system. The co-culture with *Nitratireductor* sp. demonstrated potential for enhancing biomass production, whereas the co-culture with *Sulfitobacter* sp. yielded the highest lipid levels in *Amphora* sp. during the early days of the PSBR cultivation. However, it is also important to note that certain cultures, particularly the *Amphora-Sulfitobacter* co-culture, exhibited relatively high within-group variation across different harvesting days for specific parameters, such as lipid% DW and some fatty acids (e.g., C14:0), resulting in elevated standard deviations. This variability likely reflects biological variation associated with the experimental design, as three biological replicates were conducted as independent sequential runs due to the limitation of operating a single PSBR unit. Although culture conditions (e.g., light intensity, culture medium, and temperature) were maintained consistently across runs, each replicate required the preparation of separate *Amphora* subcultures and independent microalgae-bacteria inoculations at different time points, which may have introduced batch-to-batch biological differences. Thus, increasing the number of biological replicates and

conducting co-culture experiments simultaneously in future studies will be essential to reduce within-group variability and further strengthen the robustness of these findings. On the other hand, future experiments should also explore co-cultures involving both bacterial strains and *Amphora* sp. within the PSBR. This may require shortening the disc incubation period outside the PSBR, as the fast growth of *Amphora* could accelerate its transition through growth phases once the discs are introduced into the reactor. Further optimization should also address the algae-to-bacteria ratio in order to determine the most effective balance for maximizing both biomass and lipid production. These improvements should also be accompanied by the development of more effective biofilm growth monitoring approaches, which may require improving the conversion of NDVI or other biomass proxy values into biomass by expanding calibration datasets to better capture low cell-density ranges and by applying biofilm appropriate calibration models that account for biofilm thickness, heterogeneous coverage, and pigment gradients (Hou et al., 2018; Morgado et al., 2024). For future upscale, it will be important to consider the use of more durable, reusable, and cost-effective substrate materials. The current discs occasionally detached or tore under wet conditions during handling, and biomass leakage was observed as nutrient flow eroded thicker biofilms over time. In this regard, fabric-based substrates could be a promising alternative, as they would increase the available growth area and facilitate harvesting by scraping, while allowing a portion of the biofilm to remain for continued growth without frequent re-inoculation. In addition, improvements in PSBR performance should be considered, including optimizing light distribution and efficiency while minimizing water evaporation. To better understand the chemically mediated interactions that may influence biomass and lipid production in the biofilm-based PSBR, future research will investigate metabolite exchange in *Amphora-Nitratireductor* and *Amphora-Sulfitobacter* co-cultures. Finally, long-term and continuous co-culture trials will be essential to evaluate bacterial behavioural changes over time, assess the longevity of cultivation and harvesting cycles, and ultimately determine overall operational costs.

5. Conclusion

This study evaluates binary co-cultivation of a naturally biofilm-forming benthic diatom with bacteria in a vertical porous substrate bioreactor. Our findings highlight the potential of introducing bacteria into microalgal biofilms to enable earlier attainment of higher biomass and lipid production. This strategy offers an environmentally sustainable approach that aligns with the natural characteristics of microalgal biofilms while leveraging the inherent advantages of biofilm-based cultivation. Our future research will focus on elucidating metabolite-mediated interactions in the *Amphora-Sulfitobacter* and *Amphora-Nitratireductor* co-cultures to identify key compounds contributing to enhanced biomass and lipid production of *Amphora*.

CRedit authorship contribution statement

Nadeeshani Dehel Gamage: Writing – review & editing, Writing – original draft, Visualization, Validation, Methodology, Investigation, Formal analysis, Data curation, Conceptualization. **Aurélien Mossion:** Writing – review & editing, Validation, Supervision, Investigation, Funding acquisition, Formal analysis, Conceptualization. **Murtaza Khan:** Data curation. **Rejaul Karim:** Data curation. **Vony Rabesaotra:** Methodology, Data curation. **Gaëtane Wielgosz-Collin:** Writing – review & editing, Supervision, Resources, Methodology, Funding acquisition, Conceptualization. **Thierry Lebeau:** Writing – review & editing, Supervision, Methodology, Conceptualization. **Vona Méléder:** Writing – review & editing, Validation, Supervision, Methodology, Funding acquisition, Conceptualization.

Declaration of Competing Interest

The authors declare that they have no known competing financial interests or personal relationships that could have appeared to influence the work reported in this paper.

Acknowledgements

We acknowledge financial support from the Région Pays de la Loire (France) through the SMIDAP grant BIOFILM (Agreement No. 2021_04302), the European Union under the REWRITE project (Grant Agreement 101081357), and the French Ministry of Higher Education, Research and Innovation. We are also grateful for the technical assistance of Philippe Rosa, Alexandra Petit, and Denise Jahan at the ISOMer lab for their help with autoclaving. Finally, we thank Ms. Clarisse Hubert from IFREMER (DG-ODE-PHYTOX-METALG) for her support with nutrient analyses of the samples.

Appendix A. Supporting information

Supplementary data associated with this article can be found in the online version at [doi:10.1016/j.jbiotec.2026.03.007](https://doi.org/10.1016/j.jbiotec.2026.03.007).

Data availability

Data will be made available on request.

References

- Amin, S.A., Hmelo, L.R., Van Tol, H.M., Durham, B.P., Carlson, L.T., Heal, K.R., Morales, R.L., Berthiaume, C.T., Parker, M.S., Djunaedi, B., Ingalls, A.E., Parsek, M. R., Moran, M.A., Armbrust, E.V., 2015. Interaction and signaling between a cosmopolitan phytoplankton and associated bacteria. *Nature* 522, 98–101. <https://doi.org/10.1038/nature14488>.
- Arnaldo, M.D.G., Gamage, N.D., Jaffrenou, A., Rabesaotra, V., Mossion, A., Wielgosz-Collin, G., Méléder, V., 2024a. Comparison of different small-scale cultivation methods towards the valorization of a marine benthic diatom strain for lipid production. *Algal Res.* 77, 103327. <https://doi.org/10.1016/j.algal.2023.103327>.
- Arnaldo, M.D.G., Mossion, A., Beignon, T., Vuillemin, H., Guihéneuf, F., Wielgosz-Collin, G., Méléder, V., 2024b. Diatom biofilm: ecology and cultivation from laboratory to industrial level. In: Goessling, J.W., Seródio, J., Lavaud, J. (Eds.), *Diatom photosynthesis: From primary production to high value molecules*. Wiley Scrivener, Beverly. <https://doi.org/10.1002/9781119842156.ch15>.
- Bayu, A., Rachman, A., Noerdjito, D.R., Putra, M.Y., Widayatno, W.B., 2020. High-value chemicals from marine diatoms: a biorefinery approach. *IOP Conf. Ser. Earth Environ. Sci.* 460, 012012. <https://doi.org/10.1088/1755-1315/460/1/012012>.
- Berner, F., Heimann, K., Sheehan, M., 2015. Microalgal biofilms for biomass production. *J. Appl. Phycol.* 27, 1793–1804. <https://doi.org/10.1007/s10811-014-0489-x>.
- Bligh, E.G., Dyer, W.J., 1959. A rapid method of total lipid extraction and purification. *Can. J. Biochem. Physiol.* 37 (8), 911–917. <https://doi.org/10.1139/o59-099>.
- Boukhris, S., Athmouni, K., Hamza-Mnif, I., Siala-Elleuch, R., Ayadi, H., Nasri, M., Sellami-Kamoun, A., 2017. The potential of a brown microalga cultivated in high salt medium for the production of high-value compounds. *Biomed. Res. Int.* 2017, 4018562. <https://doi.org/10.1155/2017/4018562>.
- Chandola, U., Gaudin, M., Trottier, C., Lavier-Aydat, L.J., Manirakiza, E., Menicot, S., Fischer, E.J., Louvet, I., Lacour, T., Chaumier, T., Tanaka, A., Pohnert, G., Chaffron, S., Tirichine, L., 2025. Non-cyanobacterial diazotrophs support the survival of marine microalgae in nitrogen-depleted environment. *Genome Biol.* 26, 146. <https://doi.org/10.1186/s13059-025-03597-4>.
- Cheah, Y.T., Chan, D.J.C., 2021. Physiology of microalgal biofilm: a review on prediction of adhesion on substrates. *Bioengineered* 12 (1), 7577–7599. <https://doi.org/10.1080/21655979.2021.1980671>.
- Cho, D.H., Ramanan, R., Heo, J., Lee, J., Oh, H.M., Kim, H.M., 2015. Enhancing microalgal biomass productivity by engineering a microalgal-bacterial community. *Bioresour. Technol.* 175, 578–585. <https://doi.org/10.1016/j.biortech.2014.10.159>.
- Chorazyszewski, A.M., Huang, I.S., Abdulla, H., Mayali, X., Zimba, P.V., 2021. The influence of bacteria on the growth, lipid production, and extracellular metabolite accumulation by *Phaeodactylum tricornutum* (Bacillariophyceae). *J. Phycol.* 57 (3), 931–940. <https://doi.org/10.1111/jpy.13132>.
- Cointet, E., Séverin, E., Mossion, A., Méléder, V., Gonçalves, O., Wielgosz-Collin, G., 2021. Assessment of the lipid production potential of six benthic diatom species grown in airlift photobioreactors. *J. Appl. Phycol.* 33 (4), 2093–2103. <https://doi.org/10.1007/s10811-021-02490-4>.
- Cointet, E., Wielgosz-Collin, G., Méléder, V., Gonçalves, O., 2019. Lipids in benthic diatoms: a new suitable screening procedure. *Algal Res.* 39, 101425. <https://doi.org/10.1016/j.algal.2019.101425>.
- Ennaceri, H., Ishika, T., Mkpuma, V.O., Moheimani, N.R., 2023. Microalgal biofilms: towards a sustainable biomass production. *Algal Res.* 72, 103124. <https://doi.org/10.1016/j.algal.2023.103124>.
- Fuentes, J.L., Garbayo, I., Cuaresma, M., Montero, Z., González-Del-Valle, M., Vilchez, C., 2016. Impact of microalgae-bacteria interactions on the production of algal biomass and associated compounds. *Mar. Drugs* 14, 100. <https://doi.org/10.3390/md14050100>.
- Gamage, N.D., Mossion, A., Délérès, P., Delavat, F., Tirichine, L., Rabesaotra, V., Lebeau, T., Wielgosz-Collin, G., Méléder, V., 2026. Co-culturing with bacteria modulates fatty acid composition in benthic diatom biofilms for lipid-based biotechnologies: a case study of *Amphora* sp. *Algal Res.* 93, 104449. <https://doi.org/10.1016/j.algal.2025.104449>.
- González-González, L.M., De-Bashan, L.E., 2021. Toward the enhancement of microalgal metabolite production through microalgae-bacteria consortia. *Biology* 10, 282. <https://doi.org/10.3390/biology10040282>.
- Gross, M., Henry, W., Michael, C., Wen, Z., 2013. Development of a rotating algal biofilm growth system for attached microalgae growth with in situ biomass harvest. *Bioresour. Technol.* 150, 195–201. <https://doi.org/10.1016/j.biortech.2013.10.016>.
- Gross, M., Jarboe, D., Wen, Z., 2015. Biofilm-based algal cultivation systems. *Appl. Microbiol. Biotechnol.* 99, 5781–5789. <https://doi.org/10.1007/s00253-015-6736-5>.
- Hess, D., Wendt, L.M., Wahlen, B.D., Aston, J.E., Hu, H., Quinn, J.C., 2019. Techno-economic analysis of ash removal in biomass harvested from algal turf scrubbers. *Biomass. Bioenergy* 123, 149–158. <https://doi.org/10.1016/j.biombioe.2019.02.010>.
- Hou, J., Veeragowda, D.H., van de Belt-Gritter, B., Busscher, H.J., van der Mei, H.C., 2018. Extracellular polymeric matrix production and relaxation under fluid shear and mechanical pressure in *Staphylococcus aureus* biofilms. *Appl. Environ. Microbiol.* 84, e01516-17. <https://doi.org/10.1128/AEM.01516-17>.
- Indrayani, I., Moheimani, N.R., Borowitzka, M.A., 2019. Long-term reliable culture of a halophilic diatom, *Amphora* sp. MUR258, in outdoor raceway ponds. *J. Appl. Phycol.* 31, 2771–2778. <https://doi.org/10.1007/s10811-019-01803-y>.
- Ji, X., Jiang, M., Zhang, J., Jiang, X., Zheng, Z., 2018. The interactions of algae-bacteria symbiotic system and its effects on nutrients removal from synthetic wastewater. *Bioresour. Technol.* 247, 44–50. <https://doi.org/10.1016/j.biortech.2017.09.074>.
- Kim, S., Moon, M., Kwak, M., Lee, B., Chang, Y.K., 2018. Statistical optimization of light intensity and CO₂ concentration for lipid production derived from attached cultivation of the green microalga *Etlinia* sp. *Sci. Rep.* 8, 33793. <https://doi.org/10.1038/s41598-018-33793-1>.
- Koedooder, C., Stock, W., Willems, A., Mangelincx, S., Troch, M.D., Vyverman, W., Sabbe, K., 2019. Diatom-bacteria interactions modulate the composition and productivity of benthic diatom biofilms. *Front. Microbiol.* 10, 1255. <https://doi.org/10.3389/fmicb.2019.01255>.
- Kumar, G., Shekh, A., Jakhu, S., Sharma, Y., Kapoor, R., Sharma, T.R., 2020. Bioengineering of microalgae: recent advances, perspectives, and regulatory challenges for industrial application. *Front. Bioeng. Biotechnol.* 8, 914. <https://doi.org/10.3389/fbioe.2020.00914>.
- La Peña, M.R.D., 2007. Cell growth and nutritive value of the tropical benthic diatom, *Amphora* sp., at varying levels of nutrients and light intensity, and different culture locations. *J. Appl. Phycol.* 19, 647–655. <https://doi.org/10.1007/s10811-007-9189-0>.
- Lépinay, A., Capiaux, H., Turpin, V., Mondegue, F., Lebeau, T., 2016. Bacterial community structure of the marine diatom *Haslea ostrearia*. *Algal Res.* 16, 418–426. <https://doi.org/10.1016/j.algal.2016.04.011>.
- Lépinay, A., Turpin, V., Mondegue, F., Grandet-Marchant, Q., Capiaux, H., Baron, R., Lebeau, T., 2018. First insight on interactions between bacteria and the marine diatom *Haslea ostrearia*: algal growth and metabolomic fingerprinting. *Algal Res.* 31, 395–405. <https://doi.org/10.1016/j.algal.2018.02.023>.
- Lian, J., Wijffels, R.H., Smidt, H., Sipkema, D., 2018. The effect of the algal microbiome on industrial production of microalgae. *Microb. Biotechnol.* 11, 806–818. <https://doi.org/10.1111/1751-7915.13296>.
- Lipsman, V., Shlakhter, O., Rocha, J., Segev, E., 2024. Bacteria contribute exopolysaccharides to an algal-bacterial joint extracellular matrix. *NPJ Biofilms Micro* 10, 510. <https://doi.org/10.1038/s41522-024-00510-y>.
- Liu, B., Eltanahy, E.E., Liu, H., Chua, E.T., Thomas-Hall, S.R., Wass, T.J., Pan, K., Schenk, P.M., 2020. Growth-promoting bacteria double eicosapentaenoic acid yield in microalgae. *Bioresour. Technol.* 316, 123916. <https://doi.org/10.1016/j.biortech.2020.123916>.
- Liu, T., Wang, J., Hu, Q., Cheng, P., Ji, B., Liu, J., Vhen, Y., Xhang, W., Chen, X., Chen, L., Gao, L., Ji, C., Wang, H., 2013. Attached cultivation technology of microalgae for efficient biomass feedstock production. *Bioresour. Technol.* 127, 216–222. <https://doi.org/10.1016/j.biortech.2012.09.100>.
- Llomas, A., Leon-Miranda, E., Tejada-Jimenez, M., 2023. Microalgal and nitrogen-fixing bacterial consortia: from interaction to biotechnological potential. *Plants* 12, 2476. <https://doi.org/10.3390/plants12132476>.
- Maltsev, Y., Maltseva, K., 2021. Fatty acids of microalgae: diversity and applications. *Rev. Environ. Sci. Biotechnol.* 20, 515–547. <https://doi.org/10.1007/s11157-021-09571-3>.
- Mantzorou, A., Ververidis, F., 2019. Microalgal biofilms: a further step over current microalgal cultivation techniques. *Sci. Total Environ.* 651, 3187–3201. <https://doi.org/10.1016/j.scitotenv.2018.09.355>.
- Molina-Cárdenas, C.A., Licea-Navarro, A.F., Sánchez-Saavedra, M. del P., 2020. Effects of *Vibrio cholerae* on fatty acid profiles in *Isochrysis galbana*. *Algal Res.* 46, 101802. <https://doi.org/10.1016/j.algal.2020.101802>.

- Morgado, D., Fanesi, A., Martin, T., Tebbani, S., Bernard, O., Lopes, F., 2024. Non-destructive monitoring of microalgae biofilms. *Bioresour. Technol.* 398, 130520. <https://doi.org/10.1016/j.biortech.2024.130520>.
- Nascimento, M.D., Dublan, M.A., Ortiz-Marquez, J.C.F., Curatti, L., 2013. High lipid productivity of an *Ankistrodesmus-Rhizobium* artificial consortium. *Bioresour. Technol.* 146, 400–407. <https://doi.org/10.1016/j.biortech.2013.07.085>.
- Osorio, J.H.M., Pollio, A., Frunzo, L., Lens, P.N.L., Esposito, G., 2021. A review of microalgal biofilm technologies: definition, applications, settings and analysis. *Front. Chem. Eng.* 3, 737710. <https://doi.org/10.3389/fceng.2021.737710>.
- Ouyabe, M., Kikuno, H., Tanaka, N., Babil, P., Shiwachi, H., 2019. Isolation and Identification of nitrogen-fixing bacteria associated with *Dioscorea alata* L. and *Dioscorea esculenta* L. *Microb. Resour. Syst.* 35 (1), 3–11.
- Palacios, O.A., López, B.R., de-Bashan, L.E., 2022. Microalga growth-promoting bacteria (MGPB): a formal term proposed for beneficial bacteria involved in microalgal-bacterial interactions. *Algal Res.* 61, 102585. <https://doi.org/10.1016/j.algal.2021.102585>.
- Pasquet, V., Chérouvrier, J.-R., Farhat, F., Thiéry, V., Piot, J.M., Bérard, J.B., Kaas, R., Serive, B., Patrice, T., Cadoret, J.-P., Picot, L., 2011. Study on the microalgal pigments extraction process: performance of microwave assisted extraction. *Process Biochem.* 46, 59–67. <https://doi.org/10.1016/j.procbio.2010.07.009>.
- Podola, B., Li, T., Melkonian, M., 2017. Porous substrate bioreactors: a paradigm shift in microalgal biotechnology? *Trends Biotechnol.* 35, 121–132. <https://doi.org/10.1016/j.tibtech.2016.06.004>.
- Ramanan, R., Kim, B.-H., Cho, D.-H., Oh, H.-M., Kim, H.-S., 2016. Algae-bacteria interactions: evolution, ecology and emerging applications. *Biotechnol. Adv.* 34, 14–29. <https://doi.org/10.1016/j.biotechadv.2015.12.003>.
- Rasheed, R.N., Pourbakhtiar, A., Allaf, M.M., Baharlooian, M., Rafiei, N., Aratboni, H. A., Morones-Ramirez, J.R., Winck, F.V., 2023. Microalgal co-cultivation-recent methods, trends in omics studies, applications, and future challenges. *Front. Bioeng. Biotechnol.* 11, 1193424. <https://doi.org/10.3389/fbioe.2023.1193424>.
- Rijstenbil, J.W., 2003. Effects of UVB radiation and salt stress on growth, pigments and antioxidative defense of the marine diatom *Cylindrotheca closterium*. *Mar. Ecol. Prog. Ser.* 254, 37–48. <https://doi.org/10.3354/meps254037>.
- Sapp, M., Schwaderer, A.S., Wiltshire, K.H., Hoppe, H.G., Gerds, G., Wichels, A., 2007. Species-specific bacterial communities in the phycosphere of microalgae? *Microb. Ecol.* 53, 683–699. <https://doi.org/10.1007/s00248-006-9162-5>.
- Schnurr, P.J., Allen, D.G., 2015. Factors affecting algae biofilm growth and lipid production: a review. *Renew. Sustain. Energy Rev.* 52, 418–429. <https://doi.org/10.1016/j.rser.2015.07.090>.
- Schultze, L.K.P., Simon, M.-V., Li, T., Langenbach, D., Podola, B., Melkonian, M., 2015. High light and carbon dioxide optimize surface productivity in a twin-layer biofilm photobioreactor. *Algal Res.* 8, 37–44. <https://doi.org/10.1016/j.algal.2015.01.007>.
- Sittmann, J., Bae, M., Mevers, E., Li, M., Quinn, A., Sriram, G., Clardy, J., Liu, Z., 2021. Bacterial diketopiperazines stimulate diatom growth and lipid accumulation. *Plant Physiol.* 186, 1159–1170. <https://doi.org/10.1093/plphys/kiab080>.
- Steinrücken, P., Jackson, S., Müller, O., Puntervoll, P., Kleinegris, D.M.M., 2023. A closer look into the microbiome of microalgal cultures. *Front. Microbiol.* 14, 1108018. <https://doi.org/10.3389/fmicb.2023.1108018>.
- Tong, C.Y., Honda, K., Derek, C.J.C., 2023. A review on microalgal-bacterial co-culture: the multifaceted role of beneficial bacteria towards enhancement of microalgal metabolite production. *Environ. Res.* 228, 115872. <https://doi.org/10.1016/j.envres.2023.115872>.
- Tran, H.D., Ong, B.N., Ngo, V.T., Tran, D.L., Nguyen, T.C., Tran-Thi, B.H., Do, T.T., Nguyen, T.M.L., Nguyen, X.H., Melkonian, M., 2022. New angled twin-layer porous substrate photobioreactors for cultivation of *Nannochloropsis oculata*. *Protist* 173 (6), 125914. <https://doi.org/10.1016/j.protis.2022.125914>.
- Vale, F., Sousa, C.A., Sousa, H., Simões, L.C., McBain, A.J., Simões, M., 2023. Bacteria and microalgae associations in periphyton-mechanisms and biotechnological opportunities. *FEMS Microbiol. Rev.* 47, 1–23. <https://doi.org/10.1093/femsre/fuad047>.
- Vrieze, J.D., Christiaens, M.E.R., Verstraete, W., 2017. The microbiome as engineering tool: manufacturing and trading between microorganisms. *N. Biotechnol.* 39, 206–214. <https://doi.org/10.1016/j.nbt.2017.07.001>.
- Wang, Y., Jiang, Z., Lai, Z., Yuan, H., Zhang, X., Jia, Y., Zhang, X., 2021. The self-adaptation capability of microalgal biofilm under different light intensities: photosynthetic parameters and biofilm microstructures. *Algal Res.* 58, 102383. <https://doi.org/10.1016/j.algal.2021.102383>.
- Wang, C., Tan, Y., Zhu, L., Zhou, C., Yan, X., Xu, Q., Ruan, R., Cheng, P., 2022. The intrinsic characteristics of microalgae biofilm and their potential applications in pollutants removal-a review. *Algal Res.* 68, 102849. <https://doi.org/10.1016/j.algal.2022.102849>.
- Wang, R., Xue, S., Zhang, D., Zhang, Q., Wen, S., Kong, D., Yan, C., Cong, W., 2015. Construction and characteristics of artificial consortia of *Scenedesmus obliquus*-bacteria for *S. obliquus* growth and lipid production. *Algal Res.* 12, 436–445. <https://doi.org/10.1016/j.algal.2015.10.002>.
- White, S., Anandraj, A., Bux, F., 2011. PAM fluorometry as a tool to assess microalgal nutrient stress and monitor cellular neutral lipids. *Bioresour. Technol.* 102. <https://doi.org/10.1016/j.biortech.2010.09.097>.
- Zeng, W., Chen, K., Huang, Y., Xia, A., Zhu, X., Liao, Q., 2023. Three-dimensional porous biofilm photobioreactor with light-conducting frameworks for high-efficiency microalgal growth. *Algal Res.* 69, 102942. <https://doi.org/10.1016/j.algal.2022.102942>.